Bulletin of Earthquake Engineering (2025) 23:2611–2646
https://doi.org/10.1007/s10518-025-02137-6

ORIGINAL ARTICLE

Derivation of seismic fragility curves through mechanical-analytical approaches: the case study of the URM school buildings in Friuli-Venezia Giulia region (Italy)

Sofia Giusto[1] · Ingrid Boem[2] · Sara Alfano[1] · Natalino Gattesco[2] · Serena Cattari[1]

Received: 12 November 2024 / Accepted: 27 February 2025 / Published online: 12 March 2025
© The Author(s) 2025

Abstract
Seismic events worldwide have shown that school buildings can exhibit vulnerability levels even higher than ordinary buildings. This highlights the urgent need for reliable risk analyses to guide decision-making in the implementation of large-scale mitigation policies. Developing seismic fragility curves that accurately reflect their typological and structural features is essential to achieve this. In this context, the paper compares two different mechanical-analytical methods, namely the "DBV-Masonry" and "Firstep-M_PRO", which have been independently developed at the University of Genoa and at the University of Trieste, respectively. Among various possible methods, the mechanical-analytical approach is chosen for its computational efficiency in assessing large portfolios and its flexibility in capturing the features of specific buildings, such as schools (i.e. significant inter-storey height and spacing between internal transversal walls). Both methods are applied to the same sample consisting of 101 unreinforced masonry (URM) schools located in the Friuli-Venezia Giulia region (Italy). One of key-goals of the paper is to provide a very comprehensive comparison of the similarities and differences between two methods for deriving seismic fragility curves which refer only to the global in-plane response. The impact of such an epistemic model uncertainty, together with the inter-building variability, is thus quantified and fragility curves are also validated against results from previous studies.

Keywords Unreinforced masonry school buildings · Fragility curves · Mechanical-analytical models · In-plane global response · Seismic vulnerability assessment · Regional scale

✉ Ingrid Boem
INGRID.BOEM@dia.units.it

[1] Department of Civil, Chemical and Environmental Engineering (DICCA), University of Genoa, Via Montallegro 1, Genoa 16145, Italy

[2] Department of Engineering and Architecture (DIA), University of Trieste, Piazzale Europa 1, Trieste 34173, Italy

1 Introduction

A significant part of worldwide population consists of school aged children (Alcocer et al. 2020), thus spending many time in school buildings. It is imperative to ensure the safety and security of future generations when occupying such facilities. In contrast, reconnaissance surveys after seismic events (as documented in Italy (Di Ludovico et al. 2019a, 2019b)), reveal that strategic buildings, like schools, may exhibit vulnerability levels sometimes comparable to or even higher than ordinary ones, emphasizing their crucial role in the territorial seismic risk assessment at the territorial level. Vulnerability studies conducted worldwide, such as those in Nepal (Gautam et al. 2020), Iran (Azizi-Bondarabadi et al. 2016), Chile (López-Almansa et al. 2020), Mexico (Alcocer et al. 2020) and Japan (Nakano 2020), further confirm these findings.

Recent studies, like (Carofilis et al. 2020; De Leon and Donaji 2020; González et al. 2020; Marasini et al. 2020), showcase increased attention to reducing risk and improving resilience in school buildings. Worldwide initiatives, such as (WISS 2013; UNISDR 2014; D'Ayala et al. 2020), focus on promoting "safer schools". In particular, (D'Ayala et al. 2020) focuses on enhancing school safety in developing countries through the Global Library of School Infrastructure (GLOSI), under the World Bank's Safer Schools Program. It develops tools for risk assessment, considering seismic and also floods and windstorms hazards, and offers practical tools like survey forms and a mobile app to identify vulnerable schools and plan interventions like retrofitting or relocation. The initiative (UNISDR 2014) emphasizes the importance of aligning the 2030 Agenda with the Sendai Framework to integrate Disaster Risk Reduction (DRR) into school planning. This has to be addressed by embedding DRR in the Sustainable Development Goals SDG 4 (inclusive and equitable education) and SGD 11 (inclusive, safe, resilient, and sustainable cities), and advancing resilient infrastructure and risk management; it calls for inclusive, coordinated actions among stakeholders to ensure safe, resilient schools. To conclude, (WISS 2013) highlights the Worldwide Initiative for Safe Schools (WISS), promoting political commitment, technical assistance, and knowledge-sharing to prioritize and implement global school safety initiatives.

The development and application of fragility curves is a well-recognized widespread strategy to perform reliable risk analyses and supporting decisions in large-scale risk mitigation policies (Rossetto et al. 2014; D'Ayala et al. 2015; Maio et al. 2017; Martins and Silva 2018). To provide reliable estimate, it is essential that fragility curves adequately reflect the characteristics of the specific building stock under consideration. To date, limited literature has concentrated on the fragility of school buildings and, in particular, of URM schools, although these structures are widely spread throughout the world. Valuable resources include empirical fragility curves, derived from direct damage observation, such as those for Peruvian (Muñoz et al. 2007) and Nepalese (Giordano et al. 2021b) school buildings. In Italy, the works done by (Di Ludovico et al. 2023) and (Gioiella et al. 2023) were addressed to exploit the damage data available for the school buildings stock of Abruzzo region – hit by L'Aquila earthquake in 2009 – and Central-Italy area – hit by some seismic events in 2016–2017 – to derive empirical fragility curves. However, due to their typically limited stock, these curves face the challenges of less statistically robust data compared to ordinary buildings. As a result, mechanical approaches, whether numerical or analytical models (e.g., Michel et al. 2017; D'Ayala et al. 2020; Hannewald et al. 2020; Yekrangnia et al. 2021;

Giordano et al. 2021a), have a high potential in capturing the effects of specific features influencing the seismic vulnerability of these buildings.

Recognizing the significant importance of risk and resilience assessments for the national school infrastructure, the paper presents a comparative study on the use of two mechanical-analytical based methods for assessing fragility curves of URM schools. Both of them have been adopted in the MARS (Seismic Risk Maps) project (Masi et al. 2021), that recently supported the Italian Department of Civil Protection in addressing the National Risk Assessment for the seismic risk of ordinary (Lagomarsino and Masi 2021) and school buildings (Cattari et al. 2024). In the MARS project, a consensus-based vulnerability model, integrating five methods from various research units and approaches, has been developed to define fragility curves that can serve as national-scale reference. Two of these methods are the mechanical-analytical models herein used, specifically the "DBV-Masonry" (Displacement Based Vulnerability) model and the "Firstep-M_PRO" method, developed by the University of Genoa (UniGE) (Lagomarsino and Cattari 2014) and the University of Trieste (UniTS) (Gattesco et al. 2011, 2014), respectively. Both the methods are particularly suitable for territorial-scale seismic risk assessments, due to the low computational effort and the limited number of mechanical and geometrical parameters required.

In this paper, these methods are applied to assess the seismic vulnerability of a specific sample of 101 unreinforced masonry (URM) school buildings in the Friuli-Venezia Giulia (FVG) region, in northeastern Italy, referred to as the "FVG sample". The potential of these two methods to pass from a national to a regional scale is thus investigated.

The aim of this work is to provide a detailed presentation and discussion of the two analytical-mechanical methods, highlighting their capabilities and comparing the assumptions underlying each. The results obtained from their application to the FVG sample are compared to evaluate their similarities and differences in terms of both fragility curves and territorial seismic risk assessment. The detailed content of the sections comprising the article is described below.

Section 2 offers a detailed analysis of the structural features of the FVG sample, such as construction age, number of stories, planimetric shapes, and masonry types. Additionally, it discusses the taxonomy used to classify these school buildings into sub-typologies, based on structural material, number of stories, and plan area. On these three fundamental attributes, the FVG sample is compared with data from school buildings at both regional and national scale, to assess its representativeness.

Section 3 presents a comprehensive overview of the two mechanical-analytical methods that were used to draw the fragility curves for the FVG sample. Both methods stand on the simplified calculation of the buildings capacity curves and the generation of fragility curves using a lognormal cumulative distribution, i.e. defined by median value of the intensity measure (IM_{DLi}) linked to a 50% probability of reaching the examined damage level (the Peak Ground Acceleration – PGA – in this paper), and its standard deviation (β_{DLi}). Specifically, four damage levels are considered aligned with the EMS98 scale (Grunthal 1998). The primary goal is to describe and compare the two methods, focusing on their ability to account for material and geometric nonlinearities in a building's dynamic response to an earthquake. Comparisons with detailed models, carried out with the Tremuri software (Lagomarsino et al. 2013), are also shown for four case study buildings.

Section 4 examines how the different structural parameters influence fragility curves, highlighting the importance of reliable assessments of specific parameters – such as masonry

typology, plan shape, construction age, and covered area − in determining seismic vulnerability. The overall goal is to understand the key factors that contribute to the seismic vulnerability of school buildings and, as well as to provide insights for future regional data collection and seismic risk assessments.

Section 5 compares the fragility curves obtained from the two mechanical-analytical models with each other and with those found in the literature for the Italian school building stock, particularly the fragility curves developed within the MARS-Schools project (Cattari et al. 2024), analyzing similarities and differences.

To conclude, Sect. 6 provides an example of how the vulnerability models can then be applied for the seismic risk assessment at the territorial scale, including expected damage, building usability, and related uncertainties.

2 Overview of the Italian masonry school buildings stock and description of the sample

Thanks to the collection of data on Italian school buildings that was carried out by MIUR (*Ministero dell'Istruzione e del Merito*), a database describing the school buildings in Italy is available. To date, the data have been gathered in a computerised way, and the collection of this information has been carried out by school managers or technicians appointed by the school. The AES inventory (*Anagrafe dell'Edilizia Scolastica*, i.e. the School Buildings Registry, edited by the Italian Ministry of Education in 2005 – (Portale Unico dei Dati della Scuola 2024)) reports approximately 50000 school buildings in the Country, with around 21% being masonry buildings. The distribution of the total URM school building stock by age is (Fig. 1a): 20% before 1920, 18% 1921–45, 24% 1946–60, 20% 1961–75, 8% after 1976; additionally, 10% have unknown age (NA). It is observed that, from 1976 onwards, the prevailing construction system is reinforced concrete, thus the number of masonry

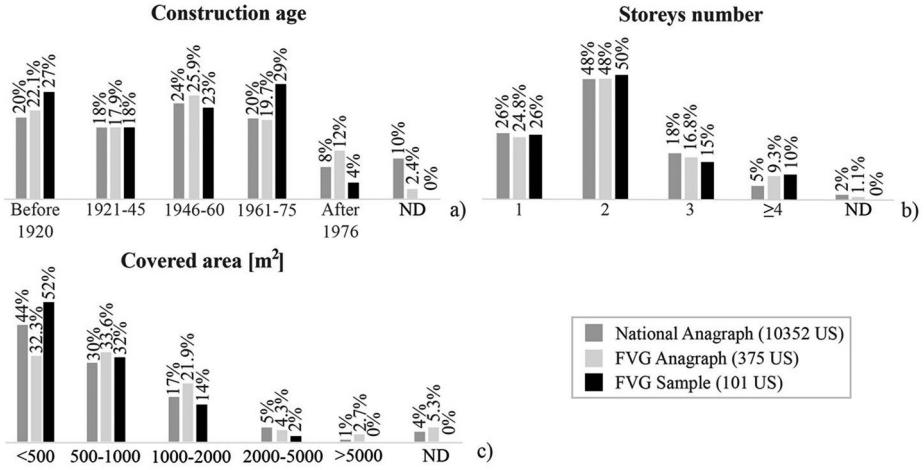

Fig. 1 Distribution of the main characteristics of the school buildings in the FVG sample (in black) and at both regional (AES_Reg, in light grey) and national (AES_Nat, in dark grey) scale, referring to the construction age (**a**), storeys number (**b**) and covered area at the ground floor (**c**). The total number of Structural Units (US) is also reported for each group

school buildings consistently decreases. Moreover, since the seismic design in Italy began gradually to take hold from 1976 (subsequently to the Friuli earthquake), it can be inferred that most of these buildings were designed only to withstand gravitational loads. Within this stock, there are different plan sizes (Fig. 1c), ranging from single-storeyed to five-storeyed URM school buildings (Fig. 1b), but the most common is the two-storeyed type with a plan area lower than 500 m^2. Also, many of these school buildings share common characteristics:

- Low-rise, with a maximum of three stories;
- Significant inter-storey height;
- Substantial distance between transverse walls (larger than URM residential buildings);
- Rigid floors;
- Elongated rectangular plans or irregular plans ("T," "L," "C" shapes, or with central courtyard or internal court).
- Internal walls with very limited openings, main façade with several openings.

The buildings sample specifically analyzed in the following to draw the fragility curves, is composed of masonry school buildings selected from the FVG regional database provided by UniTS, since detailed information on the structural characteristics is available. The database was originally prepared within the ASSESS (Analysis of Seismic Scenarios for Strategic School Buildings) research project (Grimaz et al. 2016) (2008–2011), funded by the FVG Civil Protection Agency in order to study the seismic risk of school buildings and define the intervention priorities for seismic risk reduction, considering hazard, vulnerability and exposure. Among the tasks, the project also included the collection of in-depth information concerning the structural characteristics of a group of school buildings, identified as representative of the regional asset: this consisted in both research and analysis of design documentation and on-site surveys and inspections. The collected data for each of these representative school buildings include localization, estimation of construction age and of the main interventions and subdivision into Structural Units (USs). Furthermore, each US is described by means of geometric features (walls/columns position and cross section), number and height of storeys, typology of walls/columns (including the masonry type) and of floors and roofing, with respective estimated seismic loads.

The consistency of the ASSESS database is preliminary analyzed. To this purpose, the taxonomy adopted for grouping the school buildings into sub-typologies is based on the general data available in the AES inventory, namely: structural material (e.g., reinforced concrete, masonry, steel), number of stories (i.e., 1,2,3,>4), plan area (i.e.,<500 m^2, 500–1000 m^2, 1000–2000 m^2, 2000–5000 m^2 and 5000 m^2). Moreover, sourcing from the ASSESS database, also the planimetric shape, the masonry typology, the load-bearing wall ratio and the mean inter-storey height are considered.

It is observed that the ASSESS database consists mainly of reinforced concrete and masonry school buildings, and, to a small extent, of mixed reinforced concrete-masonry school buildings. This paper examines only the structures with an exclusive or predominant masonry construction system, for a total of 101 US (i.e. the "FVG sample"). To analyze the representativeness of the FVG-sample at both the regional (AES_Reg) and national (AES_Nat) scale, a comparison is plotted in Fig. 1 (all information are taken from the AES inventory). When comparing the 101 school buildings of the FVG sample (black bars) with AES_Reg (375 schools – light grey bars), a good correlation can be observed on the number

of storeys and the age of construction; slightly different results are obtained on the covered area. When comparing the sample with AES_Nat (10352 schools – dark grey bars) a good correspondence is obtained; this denotes that the sample well reflects also the characteristics of the Italian masonry school constructions.

Table 1 gives an idea of the distribution of the 101 analyzed school buildings belonging to the FVG sample, showing the number of school buildings defining each sub-type according to number of floor and age of construction, to identify the most representative sub-types.

Figure 2 shows a graphical representation of the main sample characteristics: for the discrete parameters (plan shape and masonry type), a percentage distribution is adopted, while for the continuous, geometric parameters, a lognormal distribution is applied (characterized by a median value and a standard deviation). The choice of lognormal distribution is based on the fact the analysed values are strictly positive (so, normal distribution is not suitable).

The school buildings' distribution based on the construction age is approximately evenly distributed among the four periods before 1976 (slightly lower in 1921–1945) (Fig. 1a – black bars). The structures are mainly characterized by low 1- or 2-storeys (Fig. 1b) and are predominantly small in plan size (Fig. 1c). As far as the planimetric shape is concerned (Fig. 2a), it was noted that, in addition to the compact rectangular, quadrangular with projections and irregular planimetric shape, there are also several buildings with an elongated rectangular shape. In fact, such shape is particularly suited to school needs, allowing the arrangement of many classrooms along a corridor. Examining the prevailing masonry typology (Fig. 2b), the predominant is solid brick with lime mortar, followed by hollow brick and stone masonry, which includes different types, such as rubble stone or ashlar stone. More than 90% of the structures have reinforced concrete floors (mainly with R.C. ribs and hollow clay blocks, less frequently predalles slabs); the roof is made of similar R.C. typologies in about 75% of the buildings, but also traditional timbers roofs are found in ~ 20% cases. As it is reasonably assumed, the percentage of load-bearing walls at the ground floor in respect to the total plan area (Fig. 2c) tended to increase with the number of stories (median values, 3.5–4.6-6.2% for 1-2-≥3 storeys school buildings, respectively); however also dispersion increases with the storeys. Conversely, the median height of the ground floor results about 3.6 m, regardless of the number of stories (Fig. 2d). The ratio between the main plan dimensions (circumscribed rectangle) is often below 2 (median 1.9 m), but can sometimes be even more than doubled (elongated shape school buildings) - Fig. 2e. The small eccentricity between centers of mass and stiffness (median value = 0.27 m) indicates in many cases a balanced distribution of the load-bearing walls in plan (Fig. 2f); however, dispersion is quite large for this parameter.

For completeness, this paper is accompanied by an annex containing supplementary material. The material includes the specific characteristics of each school building analyzed, i.e. number of storeys, age of construction, ratio of x- and y-sides in plan, regularity in height, type of masonry, planimetric shape, prevailing type of floors and roofing, type of roof covering, inter-storey heights, covered area, seismic weight, percentage of resistant area and eccentricity in x-direction and y-direction.

Table 1 Sample representativeness by sub-typologies based on age of construction and number of floors

	Before 1920	1921–1945	1946–1960	1961–1975	After 1976
N1 (1-storey)	4	2	6	11	3
N2 (2-storeys)	11	10	13	15	1
N3 + (≥3-storeys)	12	6	4	3	-

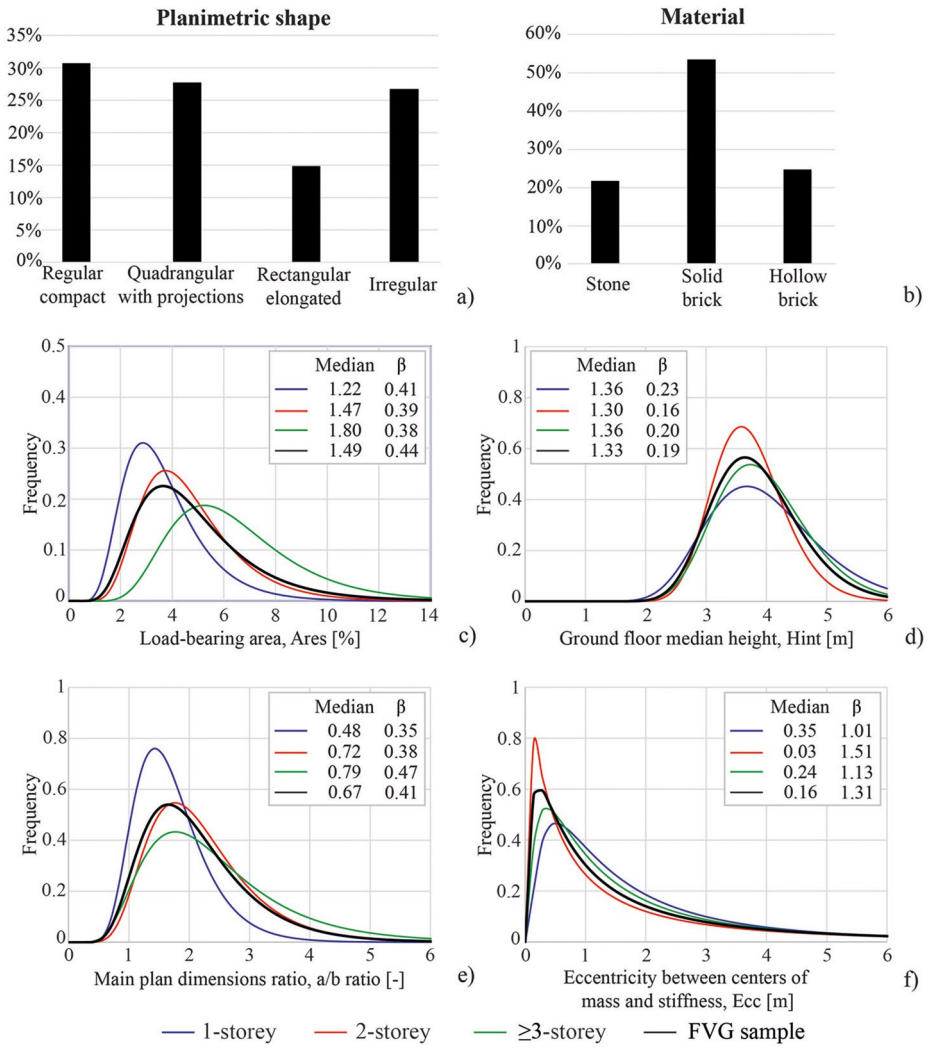

Fig. 2 Percentage distribution of the FVG sample, according to the planimetric shape (**a**) and prevailing masonry typology (**b**); lognormal distribution of the sample in terms of percentage of resistant area (**c**), inter-storey height (**d**), ratio between the two X- and Y-sides (**e**), and eccentricity (**f**). Median values and standard deviations, β, are provided for both the whole sample and as the storeys number floors varies

Figure 3 shows some case studies from the FVG sample representative of different planimetric shapes: compact (Fig. 3a), quadrangular with projections (Fig. 3b), irregular (Fig. 3c), and rectangular elongated (Fig. 3d); specifically, the four school buildings listed in the second column are later analyzed in detail, to validate and facilitate direct comparisons between the two mechanical-analytical models.

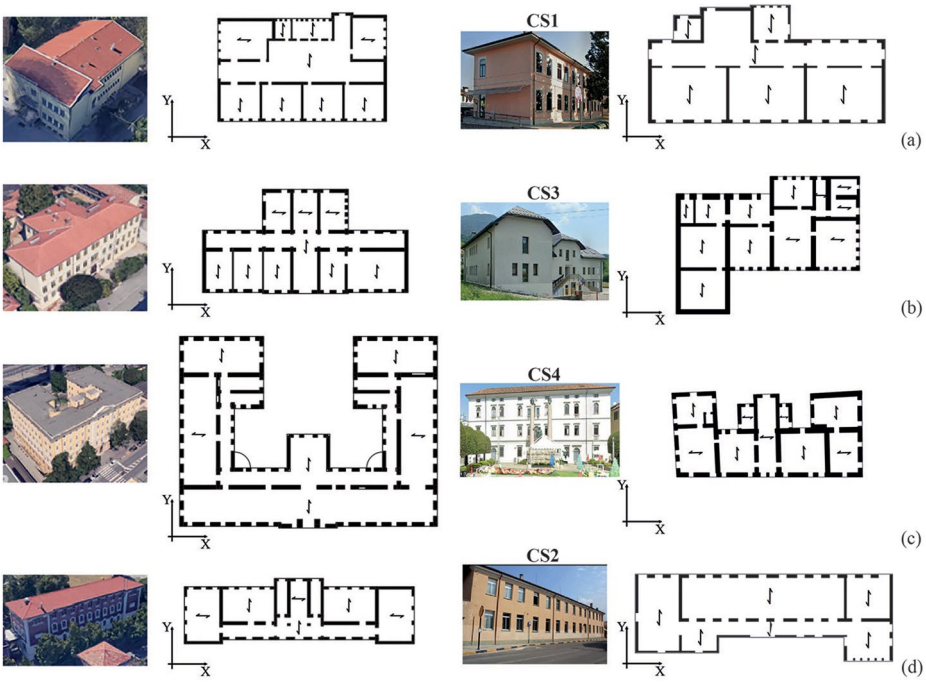

Fig. 3 Examples of different school buildings planimetric shapes: compact rectangular (**a**), quadrangular with projections (**b**), irregular (**c**) and rectangular elongated (**d**). It is observed that the four school buildings shown in the second column are the case studies analysed in detail in §3.1

3 Methods: similarities and differences between the two approaches

This section provides a detailed description of the seismic vulnerability assessment methods applied for analyzing the FVG school building sample.

It is worth to note that the two research groups worked independently, defining autonomously the procedures and analysis parameters and only sharing the same available data on school buildings; only at the end, they compared the results. Intentionally, some assumptions have not been strictly enforced to be identical in order to quantify the impact of the epistemic uncertainty inherent in different methods when applied with equally reasonable hypotheses.

To better understand the outcomes, a comprehensive overview of the main assumptions and simplifications underlying the two mechanical-analytical models adopted, named "DBV-Masonry" (Lagomarsino and Cattari 2014; Cattari et al. 2021a) and "Firstep-M_PRO" (Gattesco et al. 2011, 2014), is presented.

Both methods initially rely on the definition of a capacity curve, to which a nonlinear static procedure is then applied to derive the fragility curve. Section 3.1 delves into the fundamental principles of the two methods in defining the capacity curves, highlighting both similarities and differences; in Sect. 3.2, the comparison focuses on the derivation of the fragility curves. Both methods offer the possibility of considering the specifics of each individual structure in the sample, not only from the perspective of the mechanical properties

but also taking into account the geometric characteristics. Such information is integrated into the analytical process using data extracted from the building's floor plan. However, the level of approximation may vary, depending on the method. Regarding the DBV-Masonry model, in the context of the study here presented, it was applied using precise geometric data extracted from the floor plan, thus referring to each prototype building in the sample. As a possible alternative, the method also allows for a more flexible application without the need for a specific floor plan. In this case, representative reference parameters for a particular class of building are adopted (e.g., load-bearing areas of the masonry, average mechanical parameters, average corrective coefficients for plan irregularity), thereby reducing the complexity of the required data (Cattari and Alfano 2025a). Conversely, the Firstep-M_PRO model always requires the precise in-plan distribution of the load-bearing walls, resulting in a more accurate consideration of the specific geometric features of each analyzed building.

3.1 Definition of the capacity curves

The Firstep-M_PRO method and the DBV-Masonry model adopt a simplified mechanical-analytical procedure to determine the capacity curves for the in-plane wall response in the two main directions of the structure. They both refer to the strength of the masonry piers to determine the in-plane response of the walls. This strength depends on various factors, such as the geometry, the mechanical characteristics, the axial load, and the degree of restraint to which they are subjected, which can lead to the activation of different mechanisms, either flexural or shear.

The determination of the load bearing capacity of the masonry piers requires for both methods, the geometric description of the piers (in-plan position, length and thickness) and the identification of the masonry type(s) to assign the mechanical characteristics and self-weights. Moreover, the definition of the floors' perimeter, orientation and the identification of the floors type(s), to assign loads, is needed. Figure 4 shows the input data required for both approaches and the formulation used for the definition of base shear ($V_{b,X}$ where x indicates the direction of horizontal actions).

Starting from the fundamental principles of the mechanical response of masonry buildings, the two models implement these principles in different ways. Regarding the calculation of the base shear (V_b), the DBV-Masonry method is based on the summation of the cross-section of the masonry piers in each direction (Fig. 4 - $A_{res,x}$), considering an average vertical stress at the ground floor level (σ_{mean}). This stress accounts for the self-weight of the piers, of the floor loads, and of the spandrels weight (estimated as a percentage of the resistant area of the masonry piers). Each pier is associated with its type of masonry (i.e., mechanical parameters and specific weight), and depending on the floor type and orientation, the percentage of load absorbed by the elements in the X and Y directions is calculated. For the different types of floors, a load distribution method is defined based on the typological characteristics. For example, if the structure features a single-deck wooden floor, 90% of the weight is assigned to the load direction and the remaining 10% to the other direction; conversely, if a reinforced concrete floor with hollow blocks is present, the load is evenly distributed between the two directions. Therefore, although the DBV-Masonry method assesses the compressive stress of the masonry piers and their strength through an average value, this evaluation takes into account the presence of different types of masonry and floors. Subsequently, the shear capacity is explicitly calculated based on the Turnsek and

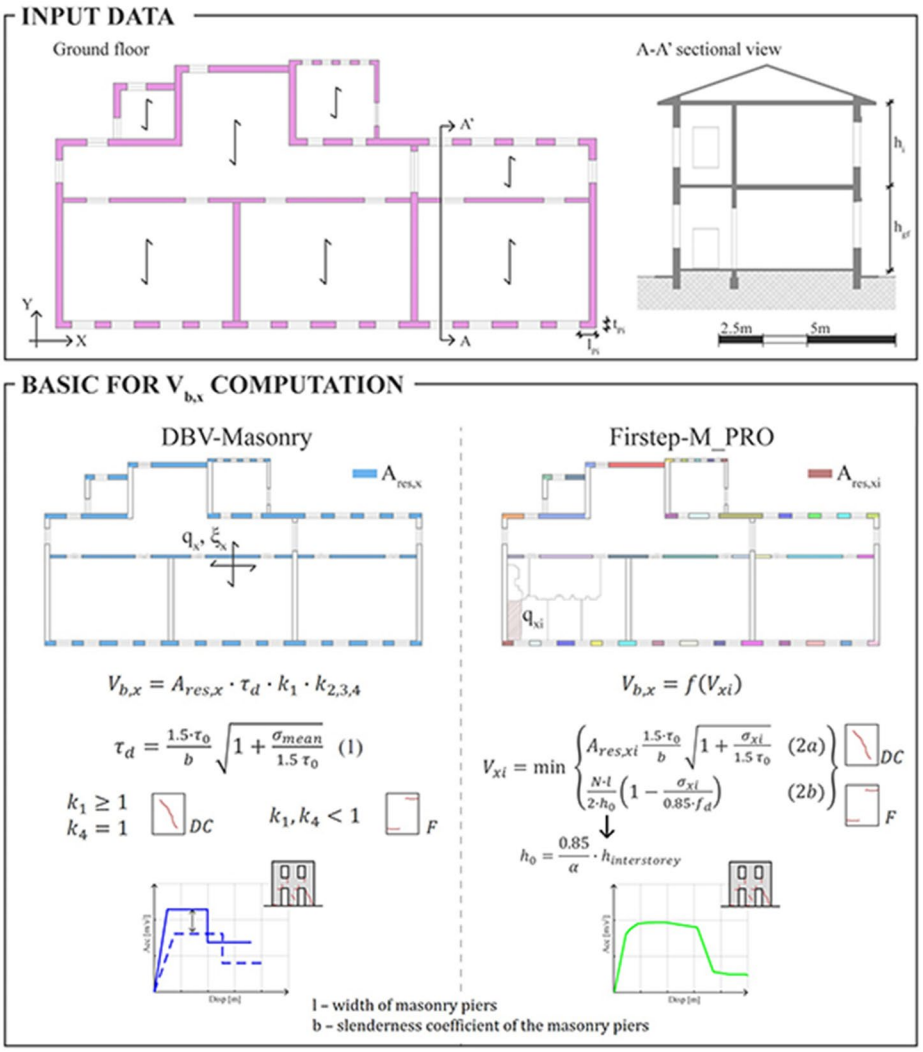

Fig. 4 Input data required for simplified mechanical-analytical models and definition of base shear (V_b) according to the two approaches

Cacovic criterion (Turnšek and Čačovič 1971), assuming $f_t = 1.5 \cdot \tau_0$ as per Circular of the Italian Structural Technical Code (Circolare 2024) (Eq. (1) in Fig. 4), that requires the definition of the shear strength of masonry (τ_d) for interpreting the diagonal cracking (DC) failure mode; the potential activation of bending mechanisms (F) is instead considered through the application of some corrective factors (k_i with i=1,..,4 (Cattari and Alfano 2025b)). Regarding the assumptions related to the static scheme of the masonry piers, specific coefficients are applied to the global base shear, based on the degree of coupling provided by the possible presence of tensile-resistant elements coupled to the spandrel beams. Specifically, the absence of elements such as reinforced concrete ring beams or tie rods (referred to as "LQD" - Low Quality Details), or the poor quality of the masonry spandrels, leads to the

definition of corrective factors that account for a dominant flexural response of the masonry piers. Conversely, the systematic presence of effective horizontal ties, such as reinforced concrete ring beams (referred to as "HQD" - High Quality Details) leads to behavior closer to the shear-type scheme; intermediate behavior is possible as well. Moreover, the capacity curve exhibits a reduction in maximum strength after reaching a severe damage state (DL3), which is calibrated as a function of quality of structural details and assumes that the mechanical capacities of the uncracked structure are compromised (Fig. 4).

On the other hand, the Firstep-M_PRO approach evaluates the normal stress acting on each pier, taking into account the masonry self-weight and the floor loads by influence area, which is automatically calculated by the tool (the load distribution ratio between bearing and unbearing walls directions can be set). Then, the in-plane lateral behavior of each pier is determined, in a simplified way, by assuming an elastic-perfectly plastic behavior till ultimate displacement (and eventually a residual strength after reaching severe damage), considering the weakest mechanism between diagonal cracking and bending (according to (NTC 2018)). In particular, the Turnsek and Cacovic criterion is applied for shear (Eq. (2a) in Fig. 4); for bending, the resistance of a cross-section without tensile strength and subjected to combined compression and bending is considered (Eq. (2b)). The total lateral force on the floor (floor shear) is the sum of the forces acting on the piers in the considered directions. It is worth to note that the in-plane lateral behavior of a pier strictly depends on its effective height and its static scheme (influenced by the coupling effect provided by spandrels). Thus, to set realistic assumptions, a series of case studies owning to the considered masonry school building database have been modeled and analyzed according to more refined methods (i.e. the Equivalent Frame method with lumped plasticity (Magenes 2000; Belmouden and Lestuzzi 2009; Raka et al. 2015; Cattari et al. 2021b)). From such analyses, it emerged that the effective pier height can be assumed, on average, approximately equal to 0.85 the inter-storey height. Besides, the bending moment distribution along the pier well accords to a shear-type scheme in single-storey school buildings (strong spandrels assumption – $\alpha=2$), while an intermediate scheme between shear-type and cantilever in case of multi-storey school buildings (partially effective spandrels – $\alpha=1.6$).

As previously introduced, both methods require the definition of reference masonry strength parameters. For the application presented in the paper, they have been assumed referring to the values proposed into the Circular of the Italian Structural Technical Code (Circolare 2024) for existing URM structures. This document recommends a range of variation for the elastic moduli and strength parameters, along with corrective factors to account for the presence of good quality of mortar, good transversal connection, etc. The procedure for determining the median value differs slightly between the two methodologies. In the DBV-Masonry model, based on the range of parameter variations proposed by the Code, the interval is adjusted according to the knowledge of the specific characteristics of the masonry by applying the corrective coefficients provided in (Circolare 2024). If information about the presence of factors that improve the masonry's behavior is not available, the corrective coefficients proposed by the technical standards are applied only to the maximum value of the range. This procedure allows for a narrower range of variation when the level of knowledge is higher. Conversely, in the cases of limited data, the lack of knowledge leads to greater uncertainty (i.e., a wider range). This range of variation is considered in calculating the dispersion of the fragility curve (see Sect. 3.2). Conversely, in the Firstep-M_PRO approach, the masonry mechanical parameters are selected in a deterministic way, starting

from the mean values suggested by the Italian technical standards and applying the corrective coefficient for good mortar, as it emerged from the inspections.

Regarding the elastic stiffness of the capacity curves, the DBV-Masonry method essentially evaluates the global shear stiffness of the system by calculating the stiffness of the equivalent oscillator explicitly accounting only for the shear component and, then, incorporating some corrective factors (namely, k_5, k_6 (Cattari and Alfano 2025b)) to account for the stiffness effects related to the flexural component and the coupling effect provided by spandrels to piers. The Firstep-M_PRO approach, on the other hand, considers both the flexural and shear contributions of each masonry pier.

Lastly, with respect to the ultimate displacement of the capacity curve, the DBV-Masonry model computes it as a combination of two basic deformed shapes, which are aimed to describe the typical failure modes: the Weak Spandrel – Strong Pier (WSSP) and Strong Spandrel – Weak Pier (SSWP). The relevance of one over the other depends on the building structural details, which affect also the dominant failure mode expected for the piers (i.e. diagonal shear failure or bending failure). Moreover, the deformed shape displacements are calculated by assuming inter-storey drift limit values differentiated by masonry type and consistent with experimental results available in the literature (Morandi et al. 2018; Rezaie et al. 2020). Additionally, the effective inter-storey height is considered to be 80% of the total inter-storey height when calculating the ultimate displacement in the case of a weak storey mechanism. Since it considers median floor values, the DBV-Masonry model performs the analysis referring to a single-degree-of-freedom system, assuming a triangular modal shape (consistent with the first vibration mode). Additionally, although in a simplified way, it also considers the eccentricity between the centers of mass and stiffness, by applying a corrective coefficient (k_3) to the structural resistance. The coefficient is estimated by using a formulation originally proposed in the Guidelines document for Seismic Risk Assessment and Reduction of Cultural Heritage (Guida 2011) or is calibrated on the basis of expert judgement, if the plan of the building analyzed is not available.

For the Firstep-M_PRO model, the ultimate displacement capacity of each pier is calculated on the basis of the weakest mechanism between shear and bending. The ultimate drift values are those suggested by the Italian technical standards (NTC 2018): 0.005 and 0.01, respectively. In addition, where the shear failure occurs, a residual strength of 80% is assumed till a drift of 0.008. Thus, once the capacity curve of every single pier is determined, the tool calculates the lateral capacity of each storey, under the hypothesis of global behavior (i.e. floors sufficiently stiff and effectively connected to the walls). So that, once the control displacement (i.e. that of the floor mass center) is known, it is possible to evaluate the actual displacement and the corresponding individual force of each pier. Operatively, once the coordinates of both center of mass and rigidity are determined, two independent analyses begin, referring to the two main directions. For each, a first elastic analysis is performed by searching for the control displacement corresponding to the first attainment of the lateral resistance in a pier (both translational and torsional contributions generated by the eccentricity are considered). Then, the analysis prosecuted by incremental steps of the control displacement: for each step, the center of rigidity and the floor rotation are iteratively updated considering the current displacement and respective force level of each pier. The floor shear is updated consequently. The floor capacity curve is obtained as the step-by-step trend of the floor shear, varying control displacement. As the direct combination of the elastic-perfectly plastic piers' capacity curves, the floor capacity curve results in a multi-

linear curve. It is characterized by an initial, linear branch, in which all the piers perform in their elastic range. As the analysis progresses, the resistance still increases and the stiffness decreases, as the different piers reach their yielding. At a certain step, the global resistance stabilizes around a nearly constant value. which is approximately maintained, resulting in a "pseudo-plastic" stage, until a pier reaches its ultimate displacement capacity, causing a global resistance reduction. The resistance reduction progresses as other piers reach their ultimate displacement. For single-storey structures, the floor capacity curve corresponds to the capacity curve of the building. Otherwise, separate analyses are conducted for each storey. Then, to evaluate the base shear associated with a generic storey, the floor shear is scaled according to a triangular distribution of the lateral forces (roughly representative of the first vibrational mode). Then, the base shear force referred to the weakest storey(s) can be selected; moreover, the displacements of the weaker storey(s) are summed to those of the over-resistant ones (assumed to behave elastically). Considering the approximation of the analysis, an almost simultaneous collapse of multiple storeys is assumed when their respective base shears differ by less than 25%. The base shear force-displacement capacity curve of the multiple degrees of freedom system is converted to one degree of freedom, assuming that the structure responds to earthquake mainly according to the first translational mode.

Once the capacity curve is calculated analytically, both methods define "target" points, that coincide with the achievement of specific Damage Levels (DLi, i = 1 … 4), intended to be consistent with the four damage levels defined by EMS-98 (Grunthal 1998): namely, slight (DL1), moderate (DL2), heavy (DL3) and very heavy (DL4) damage. For the DBV-Masonry model, DL1 and DL2 are determined based on the yield displacement (D_y) on the bilinear capacity curve and are thus directly related to the mechanical and geometric parameters on which the model is based. Specifically, DL1 corresponds to 0.7 of the yield displacement ($DL1 = 0.7*D_y$), while DL2 depends on the coefficient c_2, which varies according to the prevailing global failure mode ($DL2 = c_2*D_y$). For c_2, a value ranging from 1.1 to 2 is proposed, transitioning from the SSWP failure mode to the WSSP mode (Lagomarsino and Cattari 2014). When the predicted failure mode is SSWP, damage to the piers occurs suddenly; conversely, in the case of uniform mechanisms (WSSP), damage develops progressively in the spandrels and subsequently leads to the collapse of the piers in the final stage. This justifies positioning DL2 closer to the yield point for SSWP mechanisms and, conversely, farther away for WSSP mechanisms. Additionally, damage to the piers can significantly compromise the building's operational requirements, further justifying why DL2 is positioned closer to DL1 in the case of the SSWP failure mode. Regarding the more severe damage levels (DL3 and DL4), as aforementioned, they are calculated based on the drift limit thresholds, which differ according to the type of prevailing failure mechanism (SSWP or WSSP). The prevalence of one mechanism over the other is governed by the coefficient ε_{GFM} (Global Failure Mode), which ranges from 0.3 to 0.8 (Cattari and Alfano 2025b), with the formulations $DL3 = \varepsilon_{GFM}*DL3_{SSWP} + (1-\varepsilon_{GFM})*DL3_{WSSP}$ and similarly $DL4 = \varepsilon_{GFM}*DL4_{SSWP} + (1-\varepsilon_{GFM})*DL4_{WSSP}$. The displacement $DL_{i,WSSP}$ is calculated assuming a linear deformed shape at collapse, while the displacement $DL_{i,SSWP}$ is evaluated assuming a soft storey mechanism located at ground floor. The value of the coefficient ε_{GFM} is lower when a uniform mechanism (WSSP) is expected to activate, whereas it is higher in cases where the prevailing collapse mechanism is a soft storey (SSWP).

For the Firstep-M_PRO model, the target points are determined as follows: DL1, is assumed to be reached in the global capacity curve when a reduction of about 30% (com-

pared to the global initial stiffness) is attained; for the analyzed structures, this reflects the condition that very few piers reach the yielding point of its own capacity curve. The attainment of DL2 is associated with the beginning of the "pseudo-plastic" stage of the global curve (i.e. first point of nearly-zero tangent stiffness); it reflects the status that many the piers reached yielding. DL3 is the point where a gradual decrease in resistance starts, or the point corresponding to ¾ of the displacement where a sudden resistance decrease begins; DL4 is the point where a sudden decrease in resistance occurs, or where the residual resistance is at least 75% of the maximum resistance.

It is worth noting that both methods mechanically determine the seismic behavior of the structure by considering the in-plane response of the walls. However, the DBV-Masonry model also introduces a corrective coefficient for reducing the ductility of the structure to account for the possible premature activation of out-of-plane mechanisms in the walls (Cattari and Alfano 2025b). This method, although simplified, aims to assess how specific typological and/or morphological characteristics of the structure may allow for the activation of out-of-plane mechanisms. These reduction factors have been defined based on expert judgment, supported by empirical evidence (Sbrogiò et al. 2024) and by analytical models (Follador et al. 2023), and are applied when there are inadequate construction details and/or poor masonry characteristics that may lead to poor transverse connection quality between two orthogonal walls. Additionally, ductility reductions are also considered for certain types of floor systems that may exert thrusting actions on the walls, such as vaulted systems, or in the case of flexible floors, to account for a more limited ultimate displacement capacity due to the modest ability to redistribute actions among the walls and the possible occurrence of localized damage in individual walls. Conversely, the Firstep-M_PRO model relies on the assumption of the global response of the structure, neglecting out-of-plane failures.

Some comparisons of the capacity curves obtained from the two simplified mechanical-analytical models for four selected prototype buildings within the FVG sample are made in Fig. 5. The geometrical and typological characteristics of these school buildings are thoroughly described in (Giusto et al. 2024a). The main objective is here to assess the comparability of the results each other, despite some different underlying assumptions, and also their consistency with respect to more accurate methods to analyze the seismic capacity of the structures. In particular, the detailed modeling of these structures was performed by adopting the Equivalent Frame Modeling (EFM) and carrying out analyses by using the Tremuri software (Lagomarsino et al. 2013). Pushover non-linear static analyses have been performed by considering two load patterns (i.e. one proportional to the masses along the height – "mass"- and the other pseudo-triangular inverted miming the first modal shape – "modal"). The EFM model allows to explicitly account for several factors that a simplified mechanical-analytical model necessarily neglects or approximates, such as the effect of axial force redistribution along the analysis, the progressive damage of panels (both spandrels – that may progressively alter also the static scheme of vertical elements – and piers).

The DBV-Masonry model requires specific information about construction details that affect the effectiveness of spandrel elements to describe the structural behavior. Since such information was not always available for the FVG sample, each school building was analyzed in both "LQD" and "HQD" configuration. In the HQD case, the capacity of the spandrel elements is linked to the presence of resistant construction elements that provide tensile strength; therefore, a behavior closer to the SSWP limit case is expected. Conversely, in the absence of any tying element (LQD), a behavior closer to the WSSP limit case is likely

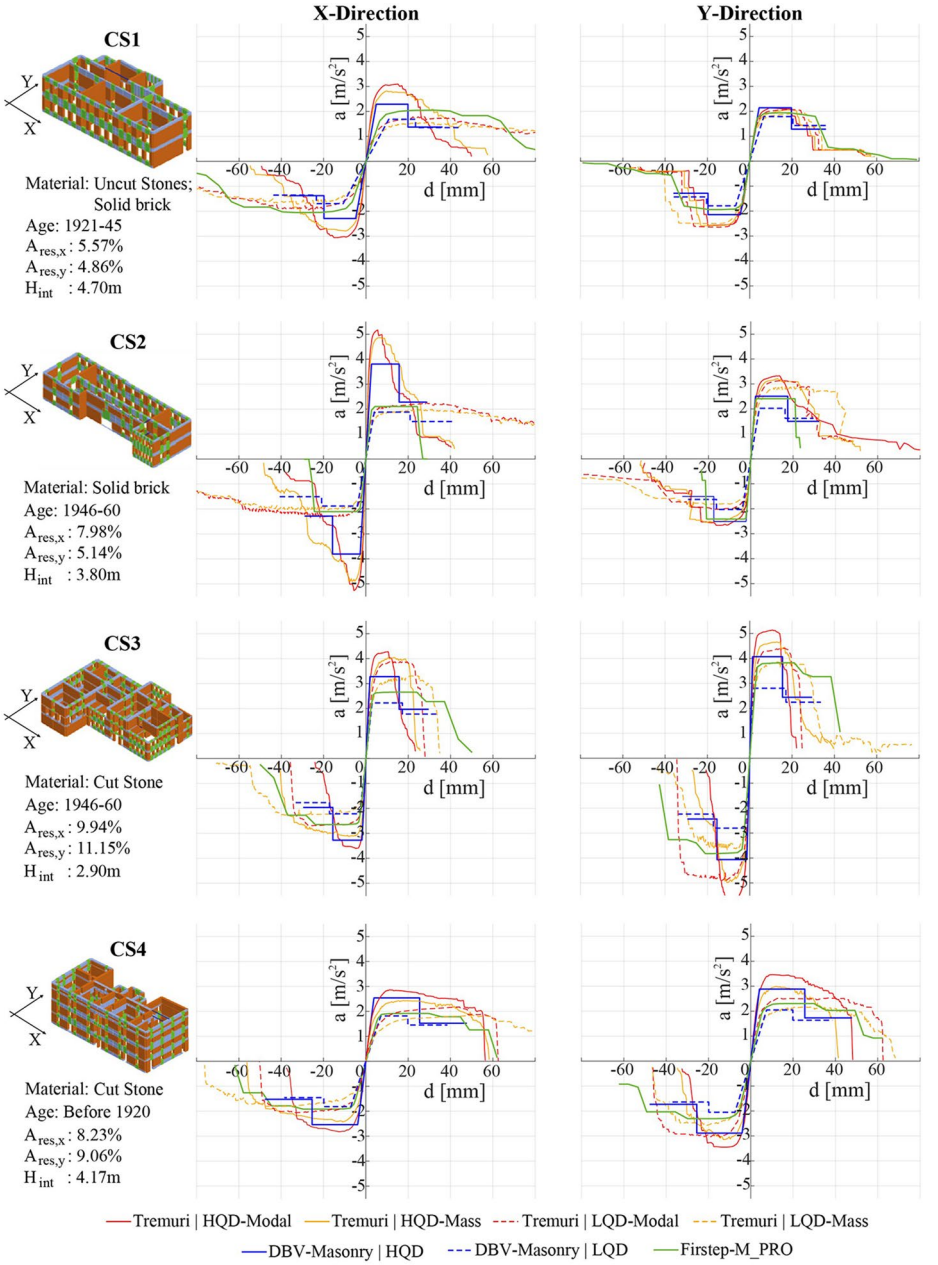

Fig. 5 Comparison in terms of capacity curves between the two simplified models (DBV-Masonry and Firstep-M_PRO) and with the capacity curves obtained from detailed models (EFM with Tremuri), for the four case study buildings. The main characteristics are also reported (3d view, material, age of construction, percentage of resistant area in x and y direction, ground floor interstorey height)

expected. In Fig. 5, for both the DBV-Masonry model and the detailed analyses with the Tremuri software, the capacity curves determined for both LQD and HQD are presented. The Firstep-M_PRO model, on the other hand, considers an intermediate condition of effective spandrels for multi-storey buildings, thus obtaining a single capacity curve.

Overall, the comparison generally shows a good agreement among the three different methods, despite the significant simplifications underlying the analytical-mechanical models in respect to the detailed three-dimensional one. The simplified models are almost always conservative compared to the curve derived from the Tremuri model, especially in terms of maximum strength. The maximum strengths obtained from the Firstep-M_PRO approach (green curves) are always in-between the HQD and LQD curves of the DBV-Masonry model (solid blue and dashed blue lines, respectively), and this is in agreement with the assumption of partially effective spandrels. Also, the stiffness of the green curves falls within the range of dotted and blue curves. In some cases, the resistance of the green curve is closer to the HQD configuration of the DBV-Masonry model, as in the Y direction of school buildings CS2 and CS3; the opposite occurs for school building CS4 and for the X direction of school building CS2. In terms of ultimate displacements, the results are in very good alignment for school buildings CS2 and CS4; quite good agreement also for school buildings CS3 and for Y direction of CS1. Higher discrepancies emerged for school building CS1 in X direction, with sensible higher values in the Firstep-M_PRO model. Actually, the damage analysis from the Tremuri software, evidenced that the failure occurs simultaneously in both floors of the structure. This is consistent with the collapse mechanism detected with the simplified Firstep-M_PRO analysis, but the approximated deformable height on which the ultimate displacement is calculated is likely overestimated in this specific case.

3.2 Definition of the fragility curves

Fragility curves describe the probability of a structure reaching or exceeding a certain level of damage, given a specific hazard intensity (such as an earthquake). The starting point for both methods in deriving seismic fragility curves is the use of the capacity curves defined for each school building in the sample (discussed in Sect. 3.1). In particular, the DBV-Masonry approach performs the analysis in the two principal directions of the structure and selects the more severe capacity curve; on the other hand, the Firstep-M_PRO method considers both curves, assuming that the direction of the seismic action is not known in advance.

Starting from the position of DLs on the capacity curve, the Intensity Measure compatible with the attainment of each DL is computed (IM_{DLi}) using a nonlinear static procedure (NSP); both methods assume as IM the Peak Ground Acceleration (PGA). The NSP allows the calculation of the maximum expected displacement demand relative to a seismic input of a certain intensity (or, vice versa, the intensity of the seismic input associated with a target displacement), using an appropriate comparison procedure between the capacity curve and a response spectrum. In the literature, two main alternative methods are proposed: the N2 method (Fajfar and Fischinger 1988), based on the use of inelastic response spectra, and the Capacity Spectrum Method (CSM) (Freeman 1998), based on the use of over-damped response spectra.

Both DBV-Masonry and Firstep-M_PRO adopt the CSM, as various results available in the literature and specifically obtained for URM structures (Marino et al. 2019; Guerrini et al. 2021; Giusto et al. 2024b), have shown that such a method provides more reliable esti-

mate than the N2 method when fragility curves obtained from nonlinear dynamic analysis (NLDA) are compared with those from nonlinear static approaches. According to Eq. (3), the use of CSM requires (i) the definition of the reference spectral shape and (ii) the determination of the damping coefficient (ξ_{DLi}) for calculating the damping correction factor that modifies the elastic spectrum.

$$IM_{DLi} = \left\{ \begin{array}{ll} \frac{D_{DLi}}{S \cdot F_0 \cdot \eta(\xi_{DLi}) \cdot \frac{T_{DLi}^2}{4\pi^2}} & T_b \leqslant T_{DLi} \leqslant T_c \\ \frac{D_{DLi}}{S \cdot F_0 \cdot \eta(\xi_{DLi}) \cdot \frac{T_{DLi}^2}{4\pi^2} \cdot \left(\frac{T_c}{T_{DLi}}\right)^{\alpha}} & T_c \leqslant T_{DLi} \leqslant T_d \end{array} \right\} \tag{3}$$

Regarding (i), the two models use for the elastic acceleration response spectrum, $S_a(T_{DLi})$, a single spectral shape compatible with that proposed by Italian technical standards (NTC 2018) for the analysis of all buildings in the sample, regardless of their actual location, and consider subsoil category A. The DBV-Masonry model uses spectral parameters derived from parametric analyses performed on response spectra obtained from real earthquake recordings (F_0=2.4 and T_c = 0.4s) and already used in a previous study (Giusto et al. 2024b). Specifically, a sensitivity study was conducted on the behavior of the descending branch of the spectrum, conventionally adopted in the Italian technical standard "at constant velocity" (thus with a proportional behavior of $1/T$ with T corresponding to the period of the structure); proportional behaviors of $(1/T)^{\alpha}$ were explored, and a value of α equal to 1.2 was defined (Smerzini et al. 2014). Differently, the Firstep-M_PRO method assumes α=1 and refers to the median spectral parameters for the national territory (F_0=2.5 and T_c = 0.33s).

Regarding (ii), different damping laws are used to assess the reduction of seismic demand based on the use of over-damped spectra: both models define the damping correction factor, $\eta(\xi_{DLi})$ - Eq. (4), as indicated by Italian technical standards, but differ in the calculation of the damping coefficient, ξ_{DLi}. The DBV-Masonry method refers to Eq. (5) and Eq. (6), depending on the predominant collapse mechanism and using coefficients specifically calibrated for URM buildings in some previous studies (Cattari and Lagomarsino 2013). Both laws refer to the system ductility (μ_{DLi}), defined as the ratio of the DL displacement to the structure's yield displacement. When the predominant collapse mechanism is uniform (i.e., the analyzed configuration is LQD), Eq. (5) applies, with $\xi_1 = 18$ and $\xi_2 = 0.8$. When the collapse is governed by weak storey (i.e, the configuration is HQD), Eq. (6) applies, with $\xi_3 = 4.5$ and $\xi_4 = 0.4$. The Firstep-M_PRO model always considers Eq. (5), with $\xi_1 = 15$ and $\xi_2 = 1$.

$$\eta\left(\xi_{DLi}\right) = \sqrt{\frac{10}{5 + \xi_{DLi}}} \geqslant 0.55 \tag{4}$$

$$\xi_{DLi} = 5 + \xi_1 \left(1 - \frac{1}{\mu_{DLi}^{\xi_2}}\right) \text{ for LQD} \tag{5}$$

$$\xi_{DLi} = \xi_3 e^{\xi_4 \mu_{DLi}} \text{ for HQD} \tag{6}$$

The differences between the two methodologies lead to variations in the definition of seismic demand, which in turn affects the estimation of the median IM_{DLi}. Additionally, the DBV-Masonry model, to account for the approximation introduced by the application of the nonlinear static procedure in calculating seismic demand, applies a multiplicative coefficient of 1.45 to the median IM value for each DL_i. This coefficient emerges from the comparison of IM estimated by static and nonlinear dynamic approaches for different damage levels, evidence discussed in (Marino et al. 2019). In (Giusto et al. 2024b), the different nonlinear static procedures, currently available in the literature, are compared, showing that the CSM methodology remains conservative relative to NLDA. The Firstep-M_PRO model does not consider this aspect.

In the process of deriving fragility curves, besides the median IM value, it is necessary to assess the propagation of uncertainties in order to define the dispersion β that allows describing the fragility curves in a lognormal format. The DBV-Masonry method accounts for the uncertainty related to the structural capacity through the response surface method (Pagnini et al. 2011), considering random variables, such as the mechanical parameters of masonry, inter-storey drift thresholds defined to assess the structural displacement capacity, floor loads, and other factors related to the knowledge of the structural geometry (inter-storey heights and the resistant areas of masonry piers). Similar approaches have been adopted in other studies available in the literature, e.g. concerning adobe masonry structures (Cocco et al. 2024), and reinforced concrete frames (Roberto et al. 2021). In the case of the FVG sample, some parameters were considered deterministic (e.g., the resistant areas of masonry piers, the inter-storey heights, the floor loads), while other parameters (the mechanical parameters of masonry) were defined by a range determined by a minimum and maximum value to account for their uncertainty. The dispersion value calculated by the model includes the intra-building variability contribution ($\beta_{intrabuilding}$), assessed through the response surface method (Pagnini et al. 2011), to which an additional dispersion contribution from the combination of fragility curves associated with different buildings ($\beta_{interbuilding}$) is added. This second contribution is determined by considering the dispersion given by the standard deviation of the IM values of the combined curves, applying the formulation shown in Eq. (7); the greater the distance between the starting curves' IM values, the higher the dispersion contribution accounting for interbuilding variability. These differences affect the reliability and accuracy of vulnerability assessments, as also noted during a 2017 expert meeting in Pavia (Silva et al. 2019), which emphasized the need for improvements in handling uncertainties, such as propagation of aleatory and epistemic uncertainties and validation of vulnerability models.

$$\beta_{interbuilding} = \sqrt{mean\left(\log(PGA_{DLi})^2\right) - (mean(\log(PGA_{DLi})))^2} \tag{7}$$

On the other hand, the Firstep-M_PRO model assumes deterministic parameters for the single building and only accounts for the interbuilding variability contribution.

The four selected case studies within the sample, already presented in Fig. 5, were also compared in terms of fragility curves. Specifically, Fig. 6 shows the comparison between the fragility curve determined by the DBV-Masonry model (the more punitive of the two principal directions), and the mean of the two IM_{DLi} derived from the Firstep-M_PRO model (X

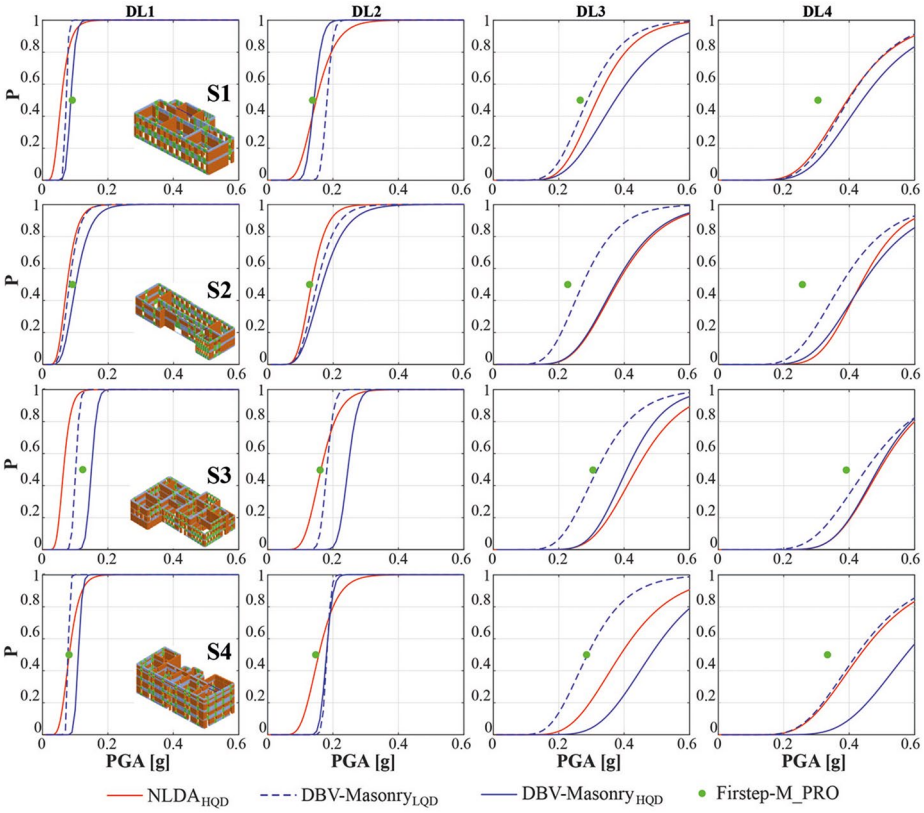

Fig. 6 Comparison of NLDAs fragility curves, under the HQD assumption, fragility curves derived from the DBV-Masonry model and the average IMs obtained by using the Firstep-M_PRO approach, evaluated for the four case study school buildings, for the different DLs

and Y directions). The Firstep-M_PRO model is thus represented with a single point of the graphs, since it does not consider any intra-building variability, as aforementioned.

In Fig. 6, the fragility curves derived from the NLDAs of the four buildings modelled with the EFM approach are also plotted (Giusto et al. 2024a). The EFM model, based on use of the Tremuri software (D'Altri et al. 2022), is capable of simulating the hysteretic behavior of the in-plane nonlinear response of panels. Due to its computational efficiency, it is particularly suitable for carrying out a large number of NLDAs, as documented in several previous works (Cattari et al. 2018; Angiolilli et al. 2021, 2023; Brunelli et al. 2022; Lagomarsino et al. 2022), together with the validation of the modelling approach (Brunelli et al. 2021; Cattari et al. 2021c). NLDAs explicitly address record-to-record variability, offering a higher level of refinement compared to simplified static methods. However, recent comparisons of fragility derivation methods reveal that while multi degrees of freedom (MDOF) non-linear time-history analyses yield the most accurate results, simplified approaches like single degrees of freedom (SDOF) systems calibrated on pushover curves or capacity spectrum methods generally underestimate median values of fragility curves and overestimate dispersion (Gentile and Galasso 2021). These biases, while significant, are within ranges

that could be corrected with appropriate calibration. The NLDAs were performed using the CLOUD + IDA approach and by selecting accelerograms as finalized in (Manfredi et al. 2022) and extensively employed in the MARS project (Masi et al. 2021; Cattari et al. 2022). The interested reader is referred to (Giusto et al. 2024a) for further details on the derivation of fragility curves from NLDA. It is noted that in the detailed modeling for NLDA, systematic reinforced concrete beams were considered at various levels of the structure; therefore, the EFM curves shown in Fig. 6 are compatible only with the HQD assumption. For the DBV-Masonry model, both the fragility curves in the LQD configuration (dashed blue lines) and those under the HQD assumption (solid blue lines) have been included in the comparison. Differently, as afore clarified, the Firstep-M_PRO results are based on the assumption of only partially effective spandrels, thus compatible with an intermediate condition.

The comparison reveals a reasonable agreement between the different methodologies, although some differences are highlighted, due to the assumptions made in deriving the fragility curves. For lower damage levels (DL1 and DL2), it is observed that the NLDA curves are slightly more vulnerable (i.e they are closer to the y-axis) compared to those obtained from the simplified approaches, especially in comparison to DBV-Masonry HQD curves. On that, it is worth mentioning also the challenging calibration of the transition from damage level 0 to damage level 1 defined in the multilinear constitutive laws used to describe the behavior of masonry piers in EFM model, which adopts secant stiffness and not a progressive degradation, thus possibly overestimating the damage in the initial phase. DL2 is defined differently on the fragility curve by the two simplified models: the Firstep-M_PRO model defines this damage level at the beginning of the plastic stage of the structure, while the DBV-Masonry model, by simplifying the capacity curve to a bilinear curve, sets DL2 at a fixed distance from the yield point (depending on the expected behavior of the structure). The comparison between the median IMs obtained from the two simplified methods, starting from DL2, is also influenced by the shape of the reference spectrum, both in terms of the "length" of the constant acceleration part (T_c value) and the reduction in demand in the DBV-Masonry method in the descending branch at constant velocity, which results in a higher IM value. However, overall, results from DBV-masonry and Firstep-M_PRO approach are consistent for DL1 and DL2. In the case of DL3 and DL4, the overall DBV-Masonry model and results from NLDA are consistent while the Firstep-M_PRO approach tends to be more conservative. For these DLs, in addition to the spectral shape, the difference in the formulation adopted for defining the damping coefficient (ξ_{DLi}) plays a more significant role. Furthermore, as previously described, the DBV-Masonry model also considers a multiplicative coefficient for the median IM to account for the reliability degree of the nonlinear static procedure compared to NLDA. Although for some structures, the differences may appear considerable, it is worth mentioning that the achieved results are compatible with the findings emerged also by other comparisons available in the literature addressed to quantify the impact of epistemic uncertainty associated with the use of various approaches (da Porto et al. 2021; Cattari et al. 2024).

Finally, regarding the dispersion of the curves, while the DBV-Masonry model in this figure accounts only for the intra-building variability, the values determined by the NLDAs account for the dispersion due to record-to-record variability. Additionally, in the case of DBV-Masonry model, the dispersion increases passing from DL1/DL2 to DL3/DL4; that depends on the fact that at DL3/DL4 the influence of dispersion on drift threshold is added to the one of masonry mechanical parameters. The latter contribution is quite moderate in

this application since it reflects the variability representative within a single building and not that of a whole building class.

Specifically, values of intra-building variability estimated by the DBV-Masonry model for the FVG sample vary from 0.06 to 0.31 for DL1/DL2 and from 0.23 to 0.32 for DL3/DL4; instead, the record-to-record variability estimated by NLDAs vary from 0.23 to 0.37. To conclude, the choice of analysis method often reflects a trade-off between simplicity and accuracy, as highlighted in recent studies (Gentile and Galasso 2021) comparing simplified and refined fragility derivation approaches.

4 Emerged trends and influence of different parameters on the seismic response of the examined buildings stock

The analysis of a specific sample of representative buildings has the advantage of considering some more detailed information that cannot be examined in large-scale analyses. Furthermore, it allows for the evaluation of the importance and influence of specific parameters, such as the number of stories or the regularity of the building plan, in defining seismic vulnerability. This section analyses the trends emerging from the FVG sample which are capable of being captured by the simplified mechanical-analytical models. Since, despite the specific differences discussed in Sect. 3, overall compatible and analogous trends were observed through two models, in this section only the outcomes of DBV-Masonry model are presented.

The results obtained for each single school building of the sample were aggregated on various parameters: type of masonry, planimetric shape, construction age and covered area. Since the sample consists of 101 school buildings, it is not sufficiently robust when divided into sub-groups based on two or three factors (such as the construction age and the number of floors at the same time). This suggests the adoption of an independent process to understand the possible influence of various parameters on the seismic vulnerability. The purpose of analyzing the different factors with the use of an independent process is to understand which parameters are eventually most important for the classification of school buildings of the sample. Such information can also be very useful for future works aimed to guide data collection on a regional scale, in order to replicate the work done on the FVG sample.

As an example, Fig. 7 highlights the variation in fragility curves for 1-storey school buildings across different masonry typologies, planimetric shapes, ages of construction, and covered areas.

In order to better investigate the significance of each analyzed parameter, Fig. 8 depicts the median PGA value across defined subgroups, with one specific parameter varying (age of construction/type of masonry/planimetric shape/covered area) alongside the number of floors (1-storey in blue, 2-storeys in red and ≥3-storeys in green). The filled symbol represents the median PGA of the analyzed group; the range of variation is also drawn (maximum and minimum limits).

Firstly, results are interpreted by referring to the trend of median values of PGA. Regarding the construction period, single-storey buildings show a significant reduction in vulnerability in more recent periods, compared to older ones (Fig. 7a). This reduction is not as evident in buildings whit two or more storeys (≥3), for which the average value of the sub-sample does not demonstrate a clear influence of this parameter (Fig. 8a). Although

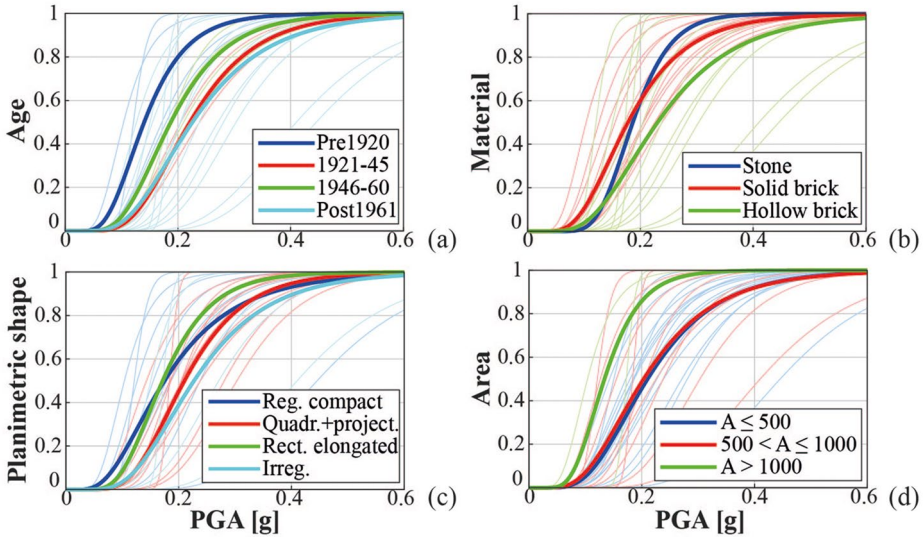

Fig. 7 Bundle of fragility curves of 1-storey school buildings varying, respectively, the age of construction (**a**), masonry typology (**b**), planimetric shape (**c**), and covered area (**d**), for DL2. Thin lines refer to individual school buildings, thick ones to the mean values for the group

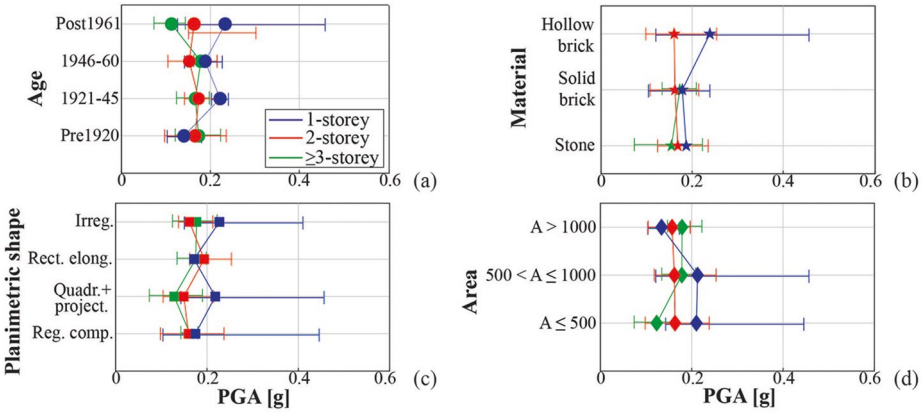

Fig. 8 Value of the median PGA and range of variation for each group, for DL2 (as example), varying the number of storeys and a parameter: (**a**) construction age, (**b**) material, (**c**) planimetric shape, and (**d**) area

the construction age has been demonstrated very relevant for discriminating the structural response of masonry buildings (Del Gaudio et al. 2021; Lagomarsino et al. 2021; Rosti et al. 2021; Scala et al. 2022; Di Ludovico et al. 2023; Cattari et al. 2024), it is not of considerable importance for this school buildings' sample because of the considerable dispersion of the results, especially for low-rise buildings. The masonry typology is also found to be more influential for single-storey buildings compared to multi-storey ones (Fig. 7a, Fig. 8a); similarly to the previous parameter, the significant dispersion of the results leads to average values that are not significantly different. Masonry type is often correlated with

the construction period and location; in fact, various periods have seen the development of different construction techniques and engineering knowledge, which, combined with available materials, have resulted in buildings with distinctive capacities and performances. A detailed analysis of the sample revealed the presence of some older school buildings (constructed before 1960) characterized by hollow brick masonry. Some studies (Messali et al. 2017; Labò et al. 2023) have pointed out the presence of hollow bricks in the earliest eras but characterized by horizontal holes that therefore have a poorer mechanical capacity and a brittle behavior compared to the modern ones. Thus, for these case studies, the mechanical parameters adopted by the DBV-Masonry model were reduced compared to those indicated by the Code (Table C8.5.I of the Circular to NTC2018), associating these masonry types with a brittle behavior, resulting in modifications to the inter-storey drift. These considerations also explain why there is a greater dispersion of individual school building results in the hollow brick type, as well as the not always evident reduction in vulnerability for this construction type.

Regarding the analysis of the planimetric shape, it revealed its significance as a determining factor. Specifically, school buildings with an elongated rectangular shape, quite numerous in the FVG sample as well as nationwide, seems performing slightly greater vulnerability (Fig. 7c); this is due to the presence of a much stronger direction than its perpendicular. Furthermore, the analysis of the planimetric shape reveals that, in general, irregular shapes tend to be not so vulnerable as expected, thanks to the increased presence of masonry elements that enhance the structure's resistant area. The analysis depicted in Fig. 8 confirms the expected trend regarding the covered area: it generally does not appear to be a fundamental parameter in defining the seismic vulnerability of masonry structures, although larger school buildings tend to be slightly more vulnerable. It should be noted by observing the dispersions in Fig. 8d, however, that there are sometimes criticalities that significantly reduce the vulnerability of the individual structure or characteristics that increase it greatly, compared to the average for a selected group, but which are not predictable except by observing the distribution of the seismic-resistant elements.

To conclude, the overall view of Fig. 8 reveals a consistent trend: vulnerability increases with the number of floors, regardless of the specific parameter under investigation.

5 Comparison of fragility curves of the two models and the literature MARS curves

In this Section, the fragility curves obtained from the two approaches for school buildings in the FVG sample are compared each other and then also with the curves available in the literature for the Italian school buildings stock, developed within the MARS-Schools project (Cattari et al. 2024).

The MARS fragility curves were derived from a combination of five different approaches: the heuristic-macroseismic approach by University of Genoa (Di Ludovico et al. 2023); the empirical-binomial approach by University of Naples Federico II (Di Ludovico et al. 2023); the Vulnus hybrid mechanical-analytical approach by University of Padua (Saler et al. 2021); the DBV-Masonry mechanical-analytical approach (Cattari et al. 2021a; Cattari and Alfano 2025a); the Firstep-M_PRO mechanical-analytical approach. The strength of the integrated MARS-Schools model lies in its ability to incorporate various approaches

in defining fragility curves, thus allowing the use of different samples of school buildings. For example, the observation-based models (the first two) were calibrated using data collected from on-site surveys carried out on school buildings in the Abruzzo region after the 2009 L'Aquila earthquake. To build up the MARS-Schools model, the Firstep-M_PRO approach was applied to the FVG sample (i.e. analogously to what presented in this paper); differently, the mechanical-analytical models DBV-Masonry and Vulnus were applied to a specific set of archetypes, selected to represent all subtypes of school buildings. Specifically, 14 prototype masonry school buildings located in various regions of Italy, belonging to different construction periods and with different geometric-structural characteristics, were selected (Cattari et al. 2021a). These buildings were first analyzed in their "as is" configuration, using specific parameters that characterize each school building in its actual state, and then re-analyzed to be representative of a class of buildings. As detailed in (Cattari et al. 2024), this procedure of extending individual prototype buildings to sub-types assumes the definition of reference values for certain parameters determined by a range of variation (e.g., the mechanical properties of the masonry, the presence of specific construction details), while other information remains unchanged to maintain the geometric-structural peculiarities of the school buildings (such as floor heights, geometric dimensions, and characteristics of plan irregularity). Coherently with the DBV-Masonry model applied to the FVG sample (Sect. 3.1), also the DBV-Masonry model applied at the national-scale analyzed both in the LQD and HQD configuration for each school building. The fragility curves obtained from the two configurations were combined based on the construction period, according to the distribution reported in Table 2. In particular, Table 2 shows the combination percentages used for the FVG sample, derived from the detailed database provided by the University of Trieste. Additionally, the values used at the national level are reported in brackets: they were derived from the average values of several national school buildings databases (sample of school buildings from the Abruzzo region, school buildings damaged following the 2016–2017 Central Italy earthquake, and the FVG sample).

Within the MARS project, the taxonomy adopted for grouping the masonry school buildings into sub-typologies considered the age of construction and the number of storeys, coherently with Table 1. For consistency in comparisons, the results obtained with the DBV-Masonry model applied to the FVG sample were aggregated without differentiating the floor area, a parameter that, however, did not significantly influence the seismic vulnerability within the FVG sample (as discussed in Sect. 4). Table 3 shows the results obtained by the two DBV-Masonry and Firstep-M_PRO models applied on the FVG sample, in terms of median PGA and dispersion β for each sub-typology; the representativeness of the sample for each subtype, relative to the 101 school buildings analyzed, is shown in Table 1 and indicated in brackets in Table 3. In aggregating the results into sub-typologies, the school buildings in the sample were considered in their "as is" state, with their structural-typological characteristics, to highlight possible effects due to regionalization.

Table 2 Combination percentages of fragility curves obtained for LQD and HQD configurations based on the construction age for the FVG sample and, in brackets, for school buildings at the national scale

	Before 1920	1921–45	1946–60	1960–75	After 1976
LQD	81% (60%)	82% (50%)	60% (40%)	4% (15%)	0% (5%)
HQD	19% (40%)	18% (50%)	40% (60%)	96% (85%)	100% (95%)

Table 3 Results obtained by the two methods (DBV-Masonry and Firstep-M_PRO) applied to the FVG sample, in terms of median PGA [g] and dispersion (β). The number of school buildings analysed for each sub-typology is also reported in brackets

Sub-typology (n° of school buildings)		DBV-Masonry				Firstep-M_PRO			
		DL1	*DL2*	*DL3*	*DL4*	*DL1*	*DL2*	*DL3*	*DL4*
N1 – Before 1920 (4)	PGA [g]	0.088	0.140	0.398	0.555	0.150	0.250	0.463	0.539
	β	0.43	0.42	0.37	0.35	0.72	0.61	0.34	0.32
N2 – Before 1920 (11)	PGA [g]	0.076	0.165	0.296	0.412	0.092	0.141	0.318	0.366
	β	0.34	0.28	0.37	0.36	0.39	0.29	0.28	0.27
N3 + – Before 1920 (12)	PGA [g]	0.078	0.173	0.275	0.400	0.102	0.161	0.309	0.362
	β	0.23	0.25	0.39	0.38	0.30	0.23	0.27	0.29
N1 – 1921/1945 (2)	PGA [g]	0.139	0.221	0.363	0.506	0.218	0.327	0.435	0.506
	β	0.42	0.41	0.37	0.34	0.13	0.13	0.08	0.10
N2 – 1921/1945 (10)	PGA [g]	0.082	0.173	0.304	0.423	0.106	0.136	0.323	0.377
	β	0.33	0.29	0.36	0.34	0.23	0.25	0.23	0.23
N3 + – 1921/1945 (6)	PGA [g]	0.074	0.166	0.264	0.376	0.093	0.141	0.247	0.296
	β	0.23	0.25	0.43	0.40	0.28	0.23	0.34	0.31
N1 – 1946/1960 (6)	PGA [g]	0.119	0.187	0.345	0.465	0.202	0.266	0.356	0.402
	β	0.42	0.42	0.38	0.35	0.40	0.36	0.22	0.20
N2 – 1946/1960 (13)	PGA [g]	0.075	0.152	0.272	0.364	0.083	0.132	0.280	0.327
	β	0.34	0.31	0.36	0.36	0.48	0.48	0.36	0.34
N3 + – 1946/1960 (4)	PGA [g]	0.091	0.178	0.294	0.415	0.102	0.161	0.308	0.363
	β	0.26	0.26	0.38	0.36	0.22	0.19	0.11	0.12
N1 – 1961/1975 (11)	PGA [g]	0.141	0.222	0.438	0.522	0.169	0.227	0.358	0.404
	β	0.44	0.44	0.36	0.36	0.33	0.33	0.19	0.18
N2 – 1961/1975 (15)	PGA [g]	0.098	0.162	0.320	0.381	0.089	0.130	0.240	0.266
	β	0.41	0.40	0.33	0.32	0.62	0.45	0.41	0.39
N3 + – 1961/1975 (3)	PGA [g]	0.057	0.112	0.259	0.355	0.063	0.128	0.197	0.223
	β	0.27	0.34	0.38	0.38	0.44	0.31	0.31	0.28
N1 – After 1976 (3)	PGA [g]	0.155	0.242	0.454	0.531	0.202	0.281	0.374	0.438
	β	0.55	0.55	0.45	0.39	0.51	0.48	0.26	0.21
N2 – After 1976 (1)	PGA [g]	0.106	0.174	0.303	0.358	0.157	0.201	0.243	0.266
	β	0.25	0.25	0.27	0.27	0.44	0.32	0.25	0.22
N3 + – After 1976(-)	PGA [g]	-	-	-	-	-	-	-	-
	β	-	-	-	-	-	-	-	-

The results obtained by the DBV-Masonry and Firstep-M_PRO models applied on the FVG sample are summarized in Table 3, in terms of media PGA and dispersion β for each sub-typology. The results indicate a reasonable agreement between the two mechanical-analytical methods, as also demonstrated in the example of Fig. 9 (blue and green curves). The Coefficient of Variation (CoV) of the median PGA is less than 15% in 64% of the cases, and exceeds 25% (but never exceeds 0.4) in only 10% of the cases. Regarding the dispersion values (β), comparable values are generally observed between the two models. As explained in Sect. 3.2, the DBV-Masonry model considers both the intra-building and inter-building variability: the two contributions are combined according to the SRSS (Square Root of the Sum of Squares) rule. Looking at the results of the DBV-Masonry model, the dispersion β, which averages around 0.36 (CoV 20%), does not appear to be influenced significantly by the specific DL, with values remaining fairly stable and CoV tending to decrease as

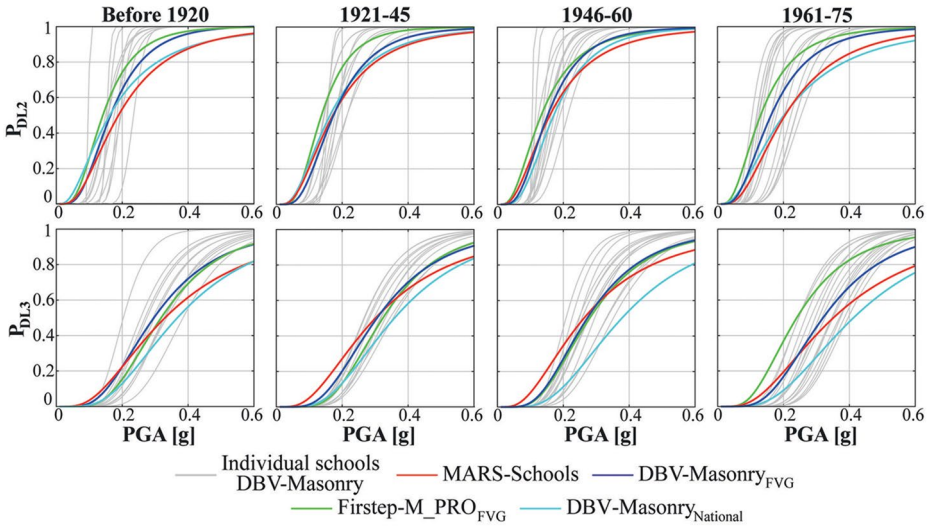

Fig. 9 Example of two-storey school buildings: fragility curves of each school building in the sample (in grey) and of the sub-typology (blue), obtained using the DBV-Masonry approach, the Firstep-M_PRO method (in green), the literature curves developed within the MARS-Schools project (Cattari et al. 2024) (in red) and the DBV-Masonry model on a national scale (in cyan), for the four different construction age and for DL2 and DL3

the damage level progresses. When applying the Firstep-M_PRO method, which considers exclusively the contribution of the inter-building variability, β averages around 0.31, but significantly higher variation emerges (CoV 43%). However, it is also observed the trend of β in decreasing as the Damage Level increases: the average is 0.36 for DL1-2 (CoV 41%) and 0.25 for DL3-4 (CoV 34%). By comparing the two models, it can thus be inferred that intra-building variability has a more marked influence on the more severe DLs.

Fig. 9 provides an example concerning the fragility curves obtained for two-storey school buildings; it compares the results obtained from the two mechanical-analytical methods applied to the FVG sample with the fragility curves determined by the integrated MARS-Schools model. Two-storey school buildings are chosen because it is the most common category within the FVG sample. The figure shows damage level 2 (DL2), representing a light damage level that impacts the operational level of the structure, and damage level 3 (DL3), which is characteristic of more severe damage. Specifically, the MARS-Schools model is represented by the red line, the Firstep-M_PRO approach in green, and the DBV-Masonry method in blue. Moreover, the curves obtained with the DBV-Masonry method for individual school buildings are plotted (thin grey lines). Additionally, the curves obtained using the DBV-Masonry method at the national scale are also shown cyan lines).

To make the fragility curve obtained from the two simplified models more comparable with those derived from the integrated MARS-Schools model, some contributions related to the uncertainty in defining the damage levels (DL_i) and the uncertainty in the seismic hazard curve have been added to the dispersion values β calculated by the two models (shown in Table 3). These contributions are accounted for through conventional values equal to 0.4 and 0.3, for DL_1/DL_2 and DL_3/DL_4, respectively, and 0.2 for the hazard curve. These values are similar to those assumed in the use of the DBV-Masonry model within the MARS

project. The combination of the different dispersion contributions was carried out using the SRSS rule.

Overall, the comparison highlights a good agreement between the different methods analyzed. Focusing on the comparison between the two simplified models used for the analysis of the FVG sample, it emerges that the Firstep-M_PRO method (green curves) yields for DL2 slightly more conservative median values compared to the DBV-Masonry approach (blue curves) across all four construction age classes shown. This result can primarily be attributed to the different definitions of the damage level on the capacity curve. In fact, the Firstep-M_PRO method defines it at the onset of the structure's plastic phase, while the DBV-Masonry model sets it at a constant distance from the yield point (see Sect. 3.1). Also for DL3 the two methods generally provide comparable results, in exception for the construction period 1961–1975, with an evident higher vulnerability predicted by the Firstep-M_PRO approach. This discrepancy is likely related to the different assumptions regarding the spandrels effectiveness in the two models. In fact, for the DBV-Masonry model, this period is mainly governed by the response of buildings characterized by HQD configuration, whereas, for earlier periods, the LQD configuration governs the response (Table 2). As emerged in previous comparisons of selected individual buildings (Figure 6), the two methods show better agreement when DBV-Masonry assumes the LQD configuration, both due to the Firstep-M_PRO model's assumption of intermediate spandrels effectiveness for all the buildings (Sect. 3.1), and to the different formulations adopted for calculating the damping coefficient (Sect. 3.2).

The comparison between the fragility curves from the two methods and those obtained from the MARS-Schools model (red curves) shows a good consistency in results, with comparable values in terms of median PGA and higher dispersions from the MARS-Schools, as likely expected, given that the latter is a combination of five different models.

Considerations on potential regionalization effects can be drawn through the comparison between the curves obtained from the DBV-Masonry model applied to the FVG sample (in blue) and at the national scale (in cyan). Especially for DL3, the results at the national scale yield less vulnerable fragility curves than those derived for the FVG sample. This is the result of studying buildings with different morphological and geometrical characteristics, as well as the different percentage combinations used to define the configuration of construction details (LQD or HQD) depending on the construction age (Table 2). Besides, it shall also be considered the greater geometric variability that is taken into account when analyzing the FVG sample (with the actual planimetric distribution of many buildings), compared to the approach adopted at the national level (identification of a smaller number of representative prototype buildings).

6 Risk assessment on the portfolio schools

The potential of the developed fragility curves is shown by carrying out a seismic risk assessment. Specifically, the IRMA platform (Italian Risk MAps) (Borzi et al. 2021) has been used to determine the expected losses for masonry school buildings in the Friuli-Venezia Giulia region. The IRMA platform is a tool developed by the EUCENTRE Foundation in collaboration with the ReLUIS consortium, to carry out damage and seismic risk analyses for various assets (such as residential, school buildings, hospitals or churches) at different

geographical scales (municipal, provincial, regional, or national). The IRMA platform was created as part of the MARS project (Masi et al. 2021) and adapted for specific use in school buildings (Cattari et al. 2024). In particular, the AES 2005 database was implemented to specialize the specific exposure of school buildings, while for seismic hazard, the MPS04 model (Stucchi et al. 2004, 2011) is used, defining hazard curves for the 9 return periods specified by Italian regulations - NTC 2018 (NTC 2018). Additionally, data from (Mori et al. 2020) is utilized to define the subsoil class of each school building site.

Figure 10 represents the map of the FVG region, where all the 344 masonry school buildings belonging to the Italian national database AES 2005 are marked in grey, while the 101 belonging to the FVG data sample are marked in red. Additionally, the figure shows the seismic hazard values for the region (expressed in median PGA [g]) provided by the MPS04 model for a 10% probability of exceedance in 50 years (475-years return period).

For the 344 FVG masonry school buildings, an intensity-based damage map was calculated, evaluating the expected level of damage following seismic events with specific return periods on a national scale. Subsequently, the simulated consequences in terms of building usability (usable, unusable for short or long periods, and collapsed) were extracted. To perform this last simulation, it was necessary to assume consequence matrices that correlate the information on the level of damage reached by each structure to its usability. For this purpose, the consequence matrices proposed in (Cattari et al. 2024), explicitly derived for masonry school buildings, were used (Table 4). They calibrated based on the usability data collected from the sample of school buildings in the Abruzzo region following the event that struck the city of L'Aquila in 2009 (Di Ludovico et al. 2023). The impact of consequence

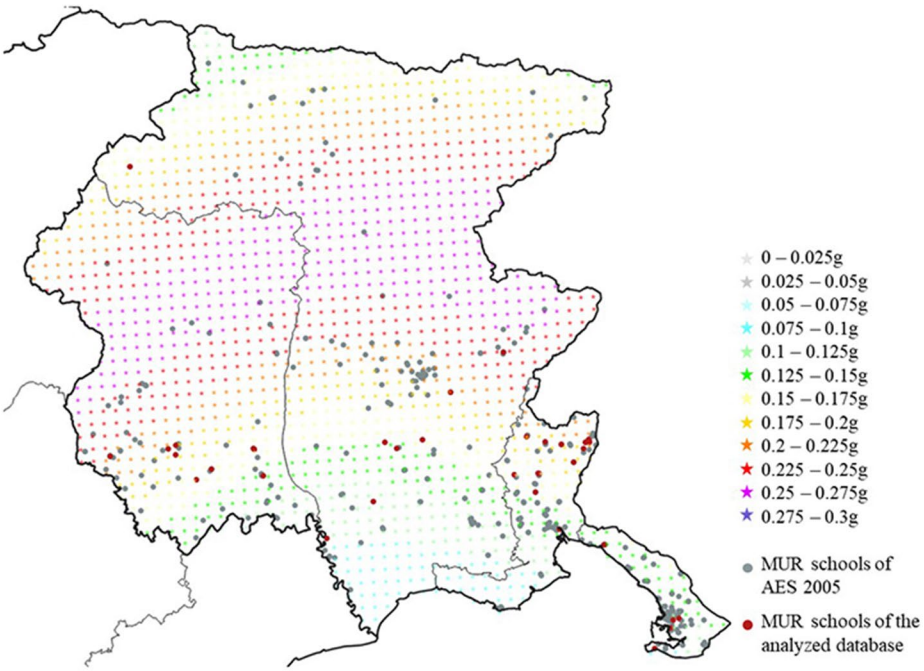

Fig. 10 Seismic hazard map of the FVG region and identification of URM school buildings from to the Italian national AES 2005 database (in grey) and those analyzed in this study belonging to the FVG data sample (in red)

Table 4 Consequence matrix defined for calculating the losses in term of usability, for URM school buildings. In brackets the values indicate those adopted in the NRA2018 for residential buildings (Dolce et al. 2021)

	Usable	Short-term unusable	Long-term unusable	Collapsed
DL1	40 (100)	50 (0)	10 (0)	0 (0)
DL2	0 (60)	33 (40)	67 (0)	0 (0)
DL3	0 (0)	20 (40)	80 (60)	0 (0)
DL4	0 (0)	0 (0)	100 (100)	0 (0)
DL5	0 (0)	0 (0)	0 (0)	100 (100)

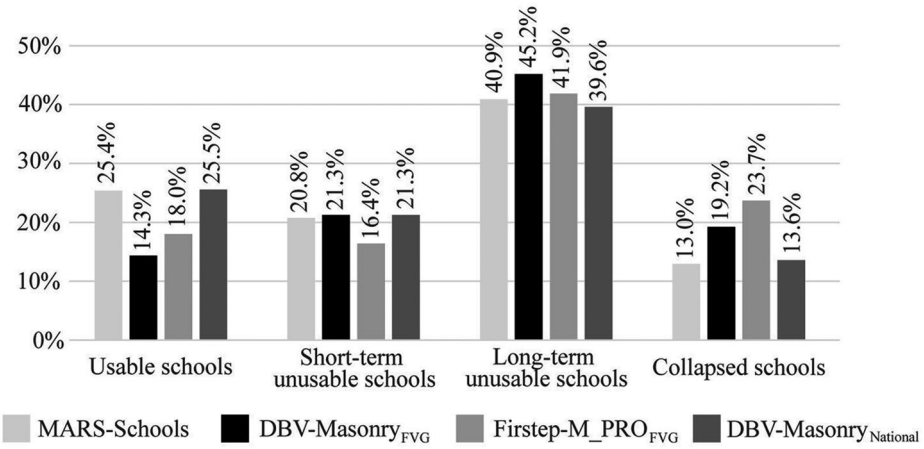

Fig. 11 Consequences, in terms of usability, for school buildings in the FVG region, obtained with the two mechanical-analytical models, the integrated MARS-Schools model and the DBV-Masonry model at a national scale, considering a 475-years return period

matrices on the final result was investigated in (Cattari et al. 2024), where a comparison is presented between the consequence matrices defined for masonry school buildings and those used for carrying out the National Risk Assessment - NRA 2018 for residential buildings (Dolce et al. 2021) (values in brackets in Table 4). From the consequence matrix shown in Table 4, buildings that reach minor damage levels (DL1 and DL2) primarily define the "usable" and "short-term unusable" buildings, while "long-term unusable" buildings are defined by 100% of the buildings that have reached severe damage levels (DL4) and by 80% of the school buildings that have reached DL3. Collapsed school buildings are defined by all structures that reach DL5. The latter is not defined by either of the two simplified models used in this work, due to the complexity of predicting structural collapse through simplified numerical methods. Therefore, to perform the risk analysis, DL5 was identified by applying a multiplicative coefficient to DL4, based on the results obtained from the macroseismic model (Lagomarsino and Giovinazzi 2006; Lagomarsino et al. 2021). Figure 11 shows the results achieved for a seismic risk analysis considering a return period of 475 years.

The result of the seismic risk analysis confirms the trend between the methods observed in Sect. 5. In particular, referring to the FVG sample, the Firstep-M_PRO model indicates a slightly higher percentage of usable school buildings than DBV-Masonry ($\Delta=+3.7\%$), and a slightly lower percentage of short-term unusable school buildings ($\Delta=-4.9\%$); but summing these two groups, the two methods almost coincide (34–36% of the structures are

included). Similarly, the Firstep-M_PRO model indicates a slightly lower percentage of long-term unusable school buildings ($\Delta = -3.3\%$), and a slightly higher percentage of collapsed school buildings ($\Delta = +4.5\%$); but, again, summing these two groups, the two methods almost coincide (64–66% of the structures are included). The DBV-Masonry model, when applied to the FVG sample (DBV-Masonry$_{FVG}$), identifies a higher vulnerability than when it is applied to the format the national-scale sample (DBV-Masonry$_{National}$). Moreover, the analysis shows good agreement between the DBV-Masonry$_{National}$ method and the integrated MARS-Schools model.

Both mechanical-analytical models presuppose some simplifications and, at this stage, is not possible conclude which is more reliable. Actually, the main goal of this detailed comparison is providing a quantitative estimate of the epistemic uncertainties intrinsic in the use of different possible approaches for such risk analyses on a territorial scale.

7 Conclusions

This study compared two mechanical-analytical methods, the DBV-Masonry model and the Firstep-M_PRO model, used to develop fragility curves for masonry school buildings in Friuli-Venezia Giulia (FVG). The application was conducted on a sample of 101 school buildings (the "FVG sample") for which detailed structural information was available.

A preliminary analysis of the database provided by the Ministry of Education (*Anagrafe dell'Edilizia Scolastica*, i.e. the School Buildings Registry, in 2005) showed that the FVG sample was representative of the region's school buildings, even though a slightly greater predominance of small buildings (< 500 m^2). The sample was proved to be representative also of the masonry school buildings at the national scale, considering the distribution in terms of construction age, storeys number and covered area.

In this context, the approaches were used to perform seismic vulnerability analysis of buildings in their actual configuration. Thus, both models initially derived the capacity curve of each structure and subsequently the fragility curves. The features of two approaches were discussed in detail. The differences in drawing the capacity curve relies at first in the determination of the base shear (with reference to the whole resistant area for DBV-Masonry, or separately, for each single resisting element, for the Firstep-M_PRO). Both methods are based on the Trunsek-Cacovic formulation for shear failure to evaluate the load-bearing resistance, but they account in different ways for the possibility of bending failure and the coupling effect of the spandrels on the piers. Different assumptions are also made for the evaluation of the initial stiffness and the ultimate displacement capacity of the structures. Once the capacity curve is drawn, the two methods apply the Capacity Spectrum Method to evaluate the peak resisting ground acceleration (PGA) associated to four Damage Levels, but differ in the definition of such DL, as well as in some response spectrum parameters and in the damping law. The differences in drawing the fragility curve are also related to dispersions: even though considering the same reference mechanical parameters for masonry, in the Firstep-M_PRO they are selected in a deterministic way, while the DBV-Masonry considers some range of variation. Moreover, the DBV-Masonry applies corrective factors to the obtained median values of PGA, to comply with the results of more accurate nonlinear dynamic analysis. The validation of the results obtained with the DBV-Masonry and Firstep-M_PRO models against those derived from nonlinear static analyses (capacity

curves) and nonlinear dynamic analyses (fragility curves) obtained from detailed models confirmed the reliability of the simplified methods.

The emerged trends and influence of different parameters on the seismic response of the sample were investigated: this analysis primarily used the DBV-Masonry model to aggregate results and compare different building characteristics, to identify which parameters impact the vulnerability and how simplified models capture these trends. This analysis did not reveal a significant influence of some specific parameters, such as the type of masonry and the planimetric shape; conversely, it was found that seismic vulnerability increases with the number of stories.

The application of the two models to the FVG sample and the comparison with the fragility curves of the MARS-School project highlighted a good agreement, although the Firstep-M_PRO model tends to provide more conservative vulnerability estimates, when considering more severe damage levels. The detailed analysis of the similarities and differences between the two methods was useful for explaining and understanding the obtained results. Overall, the results of the two models are well aligned, considering the different simplifications made. It is concluded that these simplified mechanical-analytical approaches can provide reliable estimations of the seismic response, capturing distinctive structural features with considerably lower computational effort, and this makes them an effective and efficient tool to be applied at the large territorial scale. The comparison of the results provides an estimation of the intrinsic epistemic uncertainty associated with the use of different methodologies that stem from a same type of approach (mechanical-analytical). An analogous estimation was quantified in the MARS-Schools project (Cattari et al. 2024), but in reference to different approaches (empirical, mechanical, and hybrid).

The seismic risk analysis conducted for the FVG region, using the IRMA platform, showed a good agreement between the two simplified methods, although the Firstep-M_PRO model indicated slightly higher vulnerability for losses associated with more severe damage levels, coherently with previous finding in the fragility curves. Overall, the two models suggested slight greater vulnerability compared to both the integrated MARS-School model and the DBV-Masonry model when applied at a national scale. However, such differences are more likely attributable to the different methodology, rather than a significant impact of regionalization effects on the considered building stock. This result cannot be generalized, as it is mainly a consequence of the fact that the analysed regional sample exhibits typological and constructive characteristics representative of the national stock. In other cases (e.g., in the presence of very different masonry types), the impact of regionalization is expected to be higher, and the features of the mechanical-analytical models analyzed in the paper should be able to capture this.

Supplementary information The online version contains supplementary material available at https://doi.org/10.1007/s10518-025-02137-6.

Acknowledgments This paper has been developed under the financial support of the Italian Department of Civil Protection (IDPC), within the ReLUIS-DPC 2022–2024 and 2024–2026 Research Project, which is gratefully acknowledged.

Author contributions SG: writing-original draft, data curation, conceptualization, methodology; IB: writing-original draft, data curation, conceptualization, methodology; SA: writing-original draft, data curation, conceptualization, methodology; NG: methodology, supervision, fundings; SC: writing-review, conceptualization, methodology, supervision, fundings.

Funding Open access funding provided by Università degli Studi di Trieste within the CRUI-CARE Agreement. The research activity presented in this paper, did not receive any grant from funding agencies in the public, commercial or not-for-profit sectors that may gain or lose financially through publication of this work.

Data availability The data collected for the sample of school buildings under study are resumed in the supplementary material; additional data are available under request.

Declarations

Declaration of generative AI and AI-assisted technologies in the writing process During the preparation of this work, the authors used ChatGPT to improve the English quality of the paper. After using this tool, the authors reviewed and edited the content as needed and took full responsibility for the content of the publication.

Competing interests The authors declare that they have no known competing financial interests or personal relationships that could have appeared to influence the work reported in this paper.

Open Access This article is licensed under a Creative Commons Attribution 4.0 International License, which permits use, sharing, adaptation, distribution and reproduction in any medium or format, as long as you give appropriate credit to the original author(s) and the source, provide a link to the Creative Commons licence, and indicate if changes were made. The images or other third party material in this article are included in the article's Creative Commons licence, unless indicated otherwise in a credit line to the material. If material is not included in the article's Creative Commons licence and your intended use is not permitted by statutory regulation or exceeds the permitted use, you will need to obtain permission directly from the copyright holder. To view a copy of this licence, visit http://creativecommons.org/licenses/by/4.0/.

References

Alcocer SM, Murià D, Fernández L, Ordaz M, Arce J (2020) Response of school buildings after the September 2017 earthquakes in Mexico. In: 17th World Conference on Earthquake Engineering 17WCEE. https://wcee.nicee.org/wcee/article/17WCEE/10a-0012.pdf

Angiolilli M, Brunelli A, Cattari S (2023) Fragility curves of masonry buildings in aggregate accounting for local mechanisms and site effects. Bull Earthq Eng 21(5):2877–2919. https://doi.org/10.1007/s10518-023-01635-9

Angiolilli M, Lagomarsino S, Cattari S, Degli Abbati S (2021) Seismic fragility assessment of existing masonry buildings in aggregate. Eng Struct 247(1):113218. https://doi.org/10.1016/j.engstruct.2021.113218

Azizi-Bondarabadi H, Mendes N, Lourenco P, Sadeghi N (2016) Empirical seismic vulnerability analysis for masonry buildings based on school buildings survey in Iran. Bull Earthq Eng 14. https://doi.org/10.1007/s10518-016-9944-1

Belmouden Y, Lestuzzi P (2009) An equivalent frame model for seismic analysis of masonry and reinforced concrete buildings. Constr Build Mater 23(1):40–53. https://doi.org/10.1016/j.conbuildmat.2007.10.023

Borzi B, Onida M, Faravelli M et al (2021) IRMA platform for the calculation of damages and risks of Italian residential buildings. Bull Earthq Eng 19(8). https://doi.org/10.1007/s10518-020-00924-x

Brunelli A, de Silva F, Cattari S (2022) Observed and simulated urban-scale seismic damage of masonry buildings in aggregate on soft soil: the case of Visso hit by the 2016/2017 Central Italy earthquake. Int J Disaster Risk Reduct 83:103391. https://doi.org/10.1016/j.ijdrr.2022.103391

Brunelli A, de Silva F, Piro A et al (2021)Numerical simulation of the seismic response and soil–structure interaction for a monitored masonry school building damaged by the 2016 Central Italy earthquake. Bull Earthq Eng 19(2):1181–1211. https://doi.org/10.1007/s10518-020-00980-3

Carofilis W, Perrone D, O'Reilly G, Monteiro R (2020) Filiatrault A Seismic assessment of school buildings in Italy: retrofit and risk classification. In: 17th World Conference on Earthquake Engineering 17WCEE. https://wcee.nicee.org/wcee/article/17WCEE/3g-0006.pdf

Cattari S, Alfano S (2025a) DBV-masonry dataset of mechanical-analytical fragility curves for school and residential Italian building stocks. Define Yet. Published online in submission.

Cattari S, Alfano S (2025b) DBV-Masonry model: an analytical-mechanical approach for supporting safety and risk seismic assessment of masonry buildings. Define Yet. Published online in submission

Cattari S, Alfano S, Manfredi V et al (2024) National risk assessment of Italian school buildings: the MARS project experience. Int J Disaster Risk Reduct 113:104822. https://doi.org/10.1016/j.ijdrr.2024.104822

Cattari S, Alfano S, Masi A et al (2022) Risk assessment of italian school buildings at national scale: the MARS project experience. 3rd European Conference on Earthquake Engineering & Seismology. https://hdl.handle.net/11588/908520

Cattari S, Alfano S, Ottonelli D, Saler E, da Porto F (2021a) Comparative study on two analytical mechanical-based methods for deriving fragility curves targeted to masonry school buildings. In: COMPDYN 2021 - 8th ECCOMAS Thematic Conference on Computational Methods in Structural Dynamics and Earthquake Engineering Methods in Structural Dynamics and Earthquake Engineering, p 3155–3175. https://doi.org/10.7712/120121.8703.19294

Cattari S, Camilletti D, Lagomarsino S, Bracchi S, Rota M, Penna A (2018) Masonry Italian Code-Conforming Buildings. Part 2: nonlinear Modelling and Time-History Analysis. J Earthq Eng 22(sup2):2010–2040. https://doi.org/10.1080/13632469.2018.1541030

Cattari S, Daniela C, D'Altri A, Sergio L (2021b) On the use of Continuum Finite Element and Equivalent Frame models for the seismic assessment of masonry walls. J Build Eng 43:102519. https://doi.org/10.1016/j.jobe.2021.102519

Cattari S, Degli Abbati S, Alfano S, Brunelli A, Lorenzoni F, da Porto F (2021c) Dynamic calibration and seismic validation of numerical models of URM buildings through permanent monitoring data. Earthq Eng Struct Dyn 50(10):2690–2711. https://doi.org/10.1002/eqe.3467

Cattari S, Lagomarsino S (2013) Masonry Structures. In: Sullivan T and Calvi GM Calvi Developments in the Field of Displacement Based Seismic Assessment.

Circolare. Istruzioni per l'applicazione dell'«Aggiornamento delle "Norme tecniche per le costruzioni"» di cui al decreto ministeriale 17 Gennaio 2018. G.U.S.O. n. 29 of 27/7/2018, No. 42, 21 gennaio 2019. Published online January 21, 2019. Accessed January 26,. 2024 https://www.lavoripubblici.it/normativa/20190121/Circolare-Ministero-delle-infrastrutture-e-dei-trasporti-21-gennaio-2019-n-7-18430.html

Cocco G, Spacone E, Brando G (2024) Seismic vulnerability assessment of urban areas made of adobe buildings through analytical and numerical methods: the case study of the historical center of Cusco (Peru). Int J Disaster Risk Reduct 112:104786. https://doi.org/10.1016/j.ijdrr.2024.104786

D'Altri A, Cannizzaro F, Petracca M, Talledo D (2022) Nonlinear modelling of the seismic response of masonry structures: calibration strategies. Bull Earthq Eng 20. https://doi.org/10.1007/s10518-021-01104-1

D'Ayala D, Galasso C, Nassirpour A et al (2020) Resilient communities through safer schools. Int J Disaster Risk Reduct 45:101446. https://doi.org/10.1016/j.ijdrr.2019.101446

D'Ayala D, Meslem A, Vamvatsikos D, Porter K, Rossetto T (2015) GEM Guidelines for Analytical Vulnerability Assessment of Low/Mid-Rise Buildings. Global Earthquake Model (GEM). https://doi.org/10.13117/GEM.VULN-

da Porto F, Donà M, Rosti A et al (2021)Comparative analysis of the fragility curves for Italian residential masonry and RC buildings. Bull Earthq Eng 19(8):3209–3252. https://doi.org/10.1007/s10518-021-01120-1

De Leon D, Donaji A (2020) Towards a resilient design and retrofit of schools in Mexico. In: 17th World Conference on Earthquake Engineering 17WCEE. https://wcee.nicee.org/wcee/article/17WCEE/8c-0002.pdf

Del Gaudio C, Scala SA, Ricci P, Verderame GM (2021) Evolution of the seismic vulnerability of masonry buildings based on the damage data from L'Aquila 2009 event. Bull Earthq Eng 19(11):4435–4470. https://doi.org/10.1007/s10518-021-01132-x

Di Ludovico M, Cattari S, Verderame G et al (2023) Fragility curves of Italian school buildings: derivation from L'Aquila 2009 earthquake damage via observational and heuristic approaches. Bull Earthq Eng 21(1):397–432. https://doi.org/10.1007/s10518-022-01535-4

Di Ludovico M, Digrisolo A, Moroni C et al (2019a) Remarks on damage and response of school buildings after the Central Italy earthquake sequence. Bull Earthq Eng 17. https://doi.org/10.1007/s10518-018-0332-x

Di Ludovico M, Santoro A, De Martino G et al (2019b) Cumulative damage to school buildings following the 2016 central Italy earthquake sequence. Bollettino Di Geofisica Teorica Ed Applicata 60(2):165–182. https://doi.org/10.4430/bgta0240

Dolce M, Prota A, Borzi B et al (2021) Seismic risk assessment of residential buildings in Italy. Bull Earthq Eng 19(8):2999–3032. https://doi.org/10.1007/s10518-020-01009-5

Fajfar P, Fischinger M (1988) N2-A Method for Nonlinear Seismic Analysis of Regular Buildings. In: Proceedings of the 9th World Conference on Earthquake Engineering, Vol 5, p 111–116.

Follador V, Carpanese P, Donà M et al (2023) Comparison of Fragility Sets to Assess the Effectiveness of Retrofit Interventions on Masonry Buildings in Italy. Buildings 13(12):2937. https://doi.org/10.3390/buildings13122937

Freeman S (1998) The capacity spectrum method as a tool for seismic design. In: Proceedings of 11th European conference of earthquake engineering, Paris, France.

Gattesco N, Franceschinis R, Zorzini F (2011) Metodologia per la stima della resistenza sismica degli edifici esistenti in muratura. In: ANIDIS - XIV Convegno Nazionale "L'Ingegneria Sismica in Italia". https://www.researchgate.net/publication/311370879_Metodologia_per_la_stima_della_resistenza_sismica_degli_edifici_esistenti_in_muratura

Gattesco N, Franceschinis R, Zorzini F (2014) Numerical procedure for the assessment of seismic vulnerability of masonry buildings. Int J Build Sustain Secure 1(1):35–53. https://doi.org/10.14311/BSS.2014.0005

Gautam D, Adhikari R, Rupakhety R, Koirala P (2020) An empirical method for seismic vulnerability assessment of Nepali school buildings. Bull Earthquake Eng 18(13):5965–5982. https://doi.org/10.1007/s10518-020-00922-z

Gentile R, Galasso C (2021) Simplicity versus accuracy trade-off in estimating seismic fragility of existing reinforced concrete buildings. Soil Dyn Earthq Eng 144:106678. https://doi.org/10.1016/j.soildyn.2021.106678

Gioiella L, Morici M, Dall'Asta A (2023) Empirical predictive model for seismic damage and economic losses of Italian school building heritage. Int J Disaster Risk Reduct 91:103631. https://doi.org/10.1016/j.ijdrr.2023.103631

Giordano N, De Luca F, Sextos A (2021a) Analytical fragility curves for masonry school building portfolios in Nepal. Bull Earthq Eng 19(2):1121–1150. https://doi.org/10.1007/s10518-020-00989-8

Giordano N, De Luca F, Sextos A, Ramirez Cortes F, Fonseca Ferreira C, Wu J (2021b) Empirical seismic fragility models for Nepalese school buildings. Nat Hazards 105(1):339–362. https://doi.org/10.1007/s11069-020-04312-1

Giusto S, Brunelli A, Lagomarsino S, Cattari S (2024a) Derivation of fragility curves from non linear dynamic analysis for URM buildings. Submitt Struct Elsevier. Published online

Giusto S, Cattari S, Lagomarsino S (2024b) Investigating the Reliability of Nonlinear Static Procedures for the Seismic Assessment of Existing Masonry Buildings. Appl Sci 14(3). https://doi.org/10.3390/app14031130

González C, Niño M, Jaimes MA (2020) Event-based assessment of seismic resilience in Mexican school buildings. Bull Earthq Eng 18(14):6313–6336. https://doi.org/10.1007/s10518-020-00938-5

Grimaz S, Sleiko D, Cucchi F et al (2016) The ASSESS project: assessment for seismic risk reduction of school buildings in the Friuli Venezia Giulia region (NE Italy). Boll Geofis Teor Ed Appl 57(2):111. https://doi.org/10.4430/bgta0160

Grunthal G (1998) EMS98 - European Macroseismic Scale 1998, Conseil de l'Europe -. Cahiers du Centre Européen de Géodynamique et de Séismologie, Luxemburg. Published online

Guerrini G, Kallioras S, Bracchi S, Graziotti F, Penna A (2021) Displacement demand for nonlinear static analyses of masonry structures: critical review and improved formulations. Buildings 11(3). https://doi.org/10.3390/buildings11030118

Guida L. Per la valutazione e riduzione del rischio sismico del patrimonio culturale. Published online 2011.

Hannewald P, Michel C, Lestuzzi P, Crowley H, Pinguet J, Fäh D (2020) Development and validation of simplified mechanics-based capacity curves for scenario-based risk assessment of school buildings in Basel. Eng Struct 209:110290. https://doi.org/10.1016/j.engstruct.2020.110290

Labò S, Cademartori S, Marini A (2023) Effects of the In-Plane Flexural Behavior Modeling Choices for Hollow Clay Masonry Brickwork with Horizontal Holes. Buildings 13(10):2438. https://doi.org/10.3390/buildings13102438

Lagomarsino S, Cattari S (2014) Fragility Functions of Masonry Buildings. In: Pitilakis K et al (ed) SYNER-G: typology Definition and Fragility Functions for Physical Elements at Seismic Risk, Geotechnical, Geological and Earthquake Engineering. Vol 27, p 111–156. https://doi.org/10.1007/978-94-007-7872-6_5

Lagomarsino S, Cattari S, Angiolilli M, Bracchi S, Rota M, Penna A (2022) Modelling and Seismic Response Analysis of Existing URM Structures. Part 2: archetypes of Italian Historical Buildings. J Earthq Eng 27(1):1–26. https://doi.org/10.1080/13632469.2022.2087800

Lagomarsino S, Cattari S, Ottonelli D (2021) The heuristic vulnerability model: fragility curves for masonry buildings. Bull Earthq Eng 19(4):3129–3163. https://doi.org/10.1007/s10518-021-01063-7

Lagomarsino S, Giovinazzi S (2006) Macroseismic and mechanical models for the vulnerability assessment of current buildings. Bull Earthq Eng 4:415–443. https://doi.org/10.1007/s10518-006-9024-z

Lagomarsino S, Masi A Report finale: mappe di rischio sismico dell'edilizia residenziale, Report del progetto DPC-ReLUIS 2019–2021 WP4-Mappe di rischio e scenari di danno sismico (MARS). 2021. https://www.reluis.it

Lagomarsino S, Penna A, Galasco A, Cattari S (2013) TREMURI program: an equivalent frame model for the nonlinear seismic analysis of masonry buildings. Eng Struct 56:1787–1799. https://doi.org/10.1016/j.engstruct.2013.08.002

López-Almansa F, Valdebenito G, Bustos S (2020) Observed damage at schools after the Illapel earthquake (Chile, 2015). In: 17th World Conference on Earthquake Engineering 17WCEE. https://wcee.nicee.org/wcee/article/17WCEE/3b-0008.pdf

Magenes GA (2000) method for pushover analysis in seismic assessment of masonry buildings. In: 12th World Conference on Earthquake Engineering 12WCEE, p 1–8.

Maio R, Tsionis G, Sousa M, Dimova S (2017) Review of fragility curves for seismic risk assessment of buildings in Europe. In: 16th World Conference On Earthquake Engineering 16WCEE. https://www.researchgate.net/publication/315375101_Review_of_fragility_curves_for_seismic_risk_assessment_of_buildings_in_Europe

Manfredi V, Masi A, Özcebe AG, Paolucci R, Smerzini C (2022) Selection and spectral matching of recorded ground motions for seismic fragility analyses. Bull Earthq Eng 20(10):4961–4987. https://doi.org/10.1007/s10518-022-01393-0

Marasini NP, Shrestha SN, Guragain R, Shrestha H, Prajapati R, Khatiwada P (2020) Enhancing earthquake safety of schools: lesson learned from Nepal. In: 17th World Conference on Earthquake Engineering 17WCEE. https://wcee.nicee.org/wcee/article/17WCEE/3g-0023.pdf

Marino S, Cattari S, Lagomarsino S (2019) Are the nonlinear static procedures feasible for the seismic assessment of irregular existing masonry buildings? Eng Struct 200:109700. https://doi.org/10.1016/j.engstruct.2019.109700

Martins L, Silva V A (2018) global database of vulnerability models for seismic risk assessment. In: 16th European Conference on Earthquake Engineering.

Masi A, Lagomarsino S, Dolce M, Manfredi V, Ottonelli D (2021) Towards the updated Italian seismic risk assessment: exposure and vulnerability modelling. Bull Earthq Eng 19(8):3253–3286. https://doi.org/10.1007/s10518-021-01065-5

Messali F, Metelli G, Plizzari G (2017) Experimental results on the retrofitting of hollow brick masonry walls with reinforced high performance mortar coatings. Constr Build Mater 141:619–630. https://doi.org/10.1016/j.conbuildmat.2017.03.112

Michel C, Hannewald P, Lestuzzi P, Fäh D, Husen S (2017) Probabilistic mechanics-based loss scenarios for school buildings in Basel (Switzerland). Bull Earthq Eng 15(4):1471–1496. https://doi.org/10.1007/s10518-016-0025-2

Morandi P, Albanesi L, Graziotti F, Li Piani T, Penna A, Magenes G (2018) Development of a dataset on the in-plane experimental response of URM piers with bricks and blocks. Constr Build Mater 190:593–611. https://doi.org/10.1016/j.conbuildmat.2018.09.070

Mori F, Mendicelli A, Moscatelli M, Romagnoli G, Peronace E, Naso G (2020) A new Vs30 map for Italy based on the seismic microzonation dataset. Eng Geol 275:105745. https://doi.org/10.1016/j.enggeo.2020.105745

Muñoz A, Blondet M, Aguilar R, Astorga MA (2007) Empirical Fragility Curves For Peruvian School Buildings. WIT Trans Built Environ 93:269–277

Nakano Y (2020) Damage assessment activities of school buildings after recent major earthquakes in Japan. In: 17th World Conference on Earthquake Engineering 17WCEE. https://wcee.nicee.org/wcee/article/17WCEE/8g-0004.pdf

NTC (2018) Decreto Ministeriale 17/1/2018. Norme tecniche per le costruzioni. Rome, Italy, Ministry of Infrastructures and Transportations, Published online

Pagnini L, Vicente R, Lagomarsino S, Varum H (2011) A mechanical model for the seismic vulnerability assessment of old masonry buildings. J Earthq Struct Technopress 2(1):25–42. https://doi.org/10.12989/eas.2011.2.1.025

Portale Unico dei Dati della Scuola (2024) Ministero dell'Istruzione e del Merito. August 28, 2024. https://dati.istruzione.it/opendata/

Raka E, Spacone E, Sepe V, Camata G (2015) Advanced frame element for seismic analysis of masonry structures: model formulation and validation. Earthq Eng Struct Dyn 44(14):2489–2506. https://doi.org/10.1002/eqe.2594

Rezaie A, Godio M, Beyer K (2020) Experimental Investigation of Strength, Stiffness and Drift Capacity of Rubble Stone Masonry Walls. Constr Build Mater 251:118972. https://doi.org/10.1016/j.conbuildmat.2020.118972

Roberto G, Carmine G, Stefano P (2021) Material Property Uncertainties versus Joint Structural Detailing: relative Effect on the Seismic Fragility of Reinforced Concrete Frames. J Struct Eng 147(4):04021007. https://doi.org/10.1061/(ASCE)ST.1943-541X.0002917

Rossetto T, D'Ayala D, Ioannou I, Meslem A (2014) Evaluation of Existing Fragility Curves. In: SYNER-G: typology Definition and Fragility Functions for Physical Elements at Seismic Risk. Geotechnical, Geological and Earthquake Engineering. Vol 27. Springer, p 47–93. https://doi.org/10.1007/978-94-007-7872-6_3

Rosti A, Rota M, Penna A (2021) Empirical fragility curves for Italian URM buildings. Bull Earthq Eng 19(8):3057–3076. https://doi.org/10.1007/s10518-020-00845-9

Saler E, Follador V, Carpanese P, da Porto F (2021) Fragility assessment of the Italian masonry school building asset for risk evaluation at national scale. In: COMPDYN 2021 - 8th ECCOMAS Thematic Conference on Computational Methods in Structural Dynamics and Earthquake Engineering Methods in Structural Dynamics and Earthquake Engineering, p 3113–3126. https://doi.org/10.7712/120121.8700.19014

Sbrogiò L, Saretta Y, Valluzzi MR (2024) Empirical seismic fragility of masonry buildings in historical centres accounting for structural interventions. Int J Disaster Risk Reduct 112:104757. https://doi.org/10.1016/j.ijdrr.2024.104757

Scala SA, Del Gaudio C, Verderame GM (2022) Fragility curves derivation for masonry buildings damaged after 2009 L'Aquila earthquake accounting for the effect of construction age. Int J Disaster Risk Reduct 83:103428. https://doi.org/10.1016/j.ijdrr.2022.103428

Silva V, Akkar S, Baker J et al (2019) Current Challenges and Future Trends in Analytical Fragility and Vulnerability Modeling. Earthq Spectra 35(4):1927–1952. https://doi.org/10.1193/042418EQS101O

Smerzini C, Galasso C, Iervolino I, Paolucci R (2014) Ground Motion Record Selection Based on Broadband Spectral Compatibility. Earthq Spectra 30(4):1427–1448. https://doi.org/10.1193/052312EQS197M

Stucchi M, Akinci A, Faccioli E et al (2004) Redazione Della Mappa Di Pericolosità Sismica Prevista Dall'Ordinanza PCM 3274 Del 20 Marzo 2003. Rapporto Conclusivo per Il Dipartimento Della Protezione Civile.

Stucchi M, Meletti C, Montaldo Falero V, Crowley H, Calvi G, Boschi E (2011) Seismic Hazard Assessment (2003–2009) for the Italian Building Code. Bull Seismol Soc Am 101(4):1885–1911. https://doi.org/10.1785/0120100130

Turnšek V, Čačovič F (1971) Some experimental results on the strength of brick masonry walls. In: 2nd International Brick Masonry Conference. p 149–156.

UNISDR. Comprehensive School Safety, United Nations Office for Disaster Risk Reduction (UNDRR). Published online 2014

United Nations (2024) Department of Economic and Social Affairs, Population Division. World Population Prospects. August 8, 2024. https://population.un.org/wpp/Download/

WISS. Worldwide Initiative for Safe Schools - Vision: by 2030, Every School Will Be Safe, United Nations Office for Disaster Risk Reduction (UNDRR). Published online 2013

Yekrangnia M, Bakhshi A, Ghannad MA, Panahi M (2021) Risk assessment of confined unreinforced masonry buildings based on FEMA P-58 methodology: a case study—school buildings in Tehran. Bull Earthq Eng 19(2):1079–1120. https://doi.org/10.1007/s10518-020-00990-1

Publisher's Note Springer Nature remains neutral with regard to jurisdictional claims in published maps and institutional affiliations.